AN ANALYSIS OF THE RELATION BETWEEN SOLAR RADIO EMISSION AND LARGE SOLAR COSMIC RAY INCREASES

ALEXIS SHLANTA

Research Physicist

Prepared For

RADIATION AND FIELDS BRANCH

MANNED SPACECRAFT CENTER

NATIONAL AERONAUTICS AND SPACE ADMINISTRATION

Grant NGR 44-020-001

June 1965

SCHELLENGER RESEARCH LABORATORIES

Texas Western College El Paso, Texas

ABSTRACT

15-620

A statistical analysis has been made on solar radio outbursts associated with large solar proton events. Specific criteria have been established demonstrating that solar radio outbursts are indicative of these large solar cosmic ray increases. In addition, investigations have been made into false alarms, various time relationships, mixed-frequency combinations, and possible determinations of the size of a solar proton event.

From these studies it has been found that there is a good correlation between specific signal characteristics of solar RF emission outbursts and large solar proton events. On decimeter wavelengths, these signal characteristics can be detected prior to the start of the PCA event. It has also been found that the false alarms can be considerably reduced if characteristics are specified on a combination of fixed frequencies rather than on only one frequency. In addition, there is an indication of a relationship between the area under the associated RF signal and the size of a solar proton event. Both Gold's and Parker's model of the interplanetary fields offer an explanation for some of the basic findings of this analysis.

The results of this analysis can serve as the basic criteria for an electronic system that may provide a warning for large solar proton events. Such a warning system would reduce the corpuscular radiation hazard to future space flights.

Author

ACKNOWLEDGEMENTS

The author wishes to thank Dr. Thomas G. Barnes and Professor Harold S. Slusher of Texas Western College for encouragement and many helpful suggestions. Also appreciation is extended to the following Schellenger Research Laboratories personnel for their support:

For Data Reduction:	Michael D. McAnally
For Illustrations:	James Brannon Lawrence Lyons Michael D. McAnally Thomas Taptich
For Computer Assistance:	Alfred Hulbert David Johnson
For Reproduction:	Mrs. Winifred Warder Charles Frawley Randolph Kelley
For Typing and Editing:	Mrs. Cynthia Humbert Miss Janet Lucas

TABLE OF CONTENTS

LIST OF TABLES

LIST OF ILLUSTRATIONS

INTRODUCTION

In recent years, our knowledge of solar activity has been greatly increased due to the development of radio astronomy. The sun has been successfully monitored at radio wavelengths since 1955. At present, the sun is being continuously watched twenty-four hours a day over a wide band of frequencies. Large outbursts of solar RF emission are detected periodically. These solar radio outbursts are only one of the many events associated with solar flares.

The ability of the sun to produce large bursts of energetic particles has been studied in detail since 1956. These solar particle increases, which occur in conjunction with large optical flares, are due to violent ejections from the sun at irregular intervals. Inasmuch as solar cosmic ray increases are composed primarily of protons, these phenomena are referred to as solar proton events. Large solar proton events are defined as having integrated omnidirectional flux greater than or equal to 10^7 protons/cm^2 at energies greater than 30 Mev.

Large outbursts of radio wave emission from the sun are universally recognized by several noted workers in the field[1-11] to be associated with proton events. International Geophysical Year (IGY) studies have shown that there is a close connection between spectral type-IV bursts, originating in the solar atmosphere, and solar cosmic ray increases at the earth.

The purpose of this report is:

A. To present a new approach to the study of the relation between solar radio emission and large solar proton events.

B. To present the results of this study and show how it adds new information to the relation between these solar phenomena, and

C. To show the practical significance of the results.

Initially, in this study, associated solar RF emission outbursts on fixed-frequency records have been carefully selected for each large proton event that has been measured at the earth from 1956 to the present. These RF outbursts have been studied for characteristics which might be related to solar proton events. Specific criteria have been established demonstrating that solar radio outbursts are indicative of these large solar cosmic ray increases. These criteria are concerned with the characteristics of both type II and type IV solar radio emission.

After criteria were established for solar radio emission to be indicative of large solar proton events, additional studies have been made. These studies include the investigation of false alarms, various time relationships, mixed frequency combinations, and possible proton event size determinations. A false alarm is defined as a case when a characteristic solar radio emission signal is received, but no large associated solar cosmic ray increase is observed at the earth. Various time studies have been made to determine whether or not pertinent characteristics of the solar RF emission outbursts actually precede the start of the proton increase at the earth. The characteristics of mixed fixed-frequency combinations have been investigated for more reliable indications of large solar proton events. Finally, studies have been made into possible proton event size (integrated omnidirectional flux) determinations by using the associated RF emission outbursts.

There is a good correlation between specific signal characteristics of solar RF emission outbursts and large solar cosmic ray increases. On decimeter wavelengths, these signal characteristics can be detected prior to arrival of energetic protons from the sun. The false alarms can be considerably reduced by specifying characteristics on a combination of fixed frequencies rather than on only one

frequency. There is an indication of a relationship when specific characteristics of outstanding solar RF bursts are compared with proton event size. Both Gold's and Parker's model of the interplanetary space offer an explanation for some of the basic findings of the analysis.

Large solar cosmic ray increases are a danger to manned space flight. If an intense event is encountered in space, it could cause component breakdown, incapacitation and/or death to space travelers, thus resulting in complete mission failure. The proton event hazard can be considerably reduced if a warning is provided prior to the arrival of energetic particles from the sun. The results presented in this report can serve as the basic criteria for an electronic system that may provide such a warning.

PROCEDURE

Ample data has been obtained to make this study of the relationship between solar radio emission and large solar cosmic ray increases. A reference period from 1956-1961 has been used for this study. This period coincides with the maximum phase of solar cycle 19.

The basic source of solar RF emission data has been the International Astronomical Union (IAU) Quarterly Bulletins of Solar Activity from 1956 to 1961. The IAU Bulletins are published by the Eidgen Sternwarte in Zurich, Switzerland, with financial support from UNESCO. The data published in the IAU Quarterlies are compiled from data submitted by radio observatory locations all over the world. For a list of these observing stations, as of December, 1961, see Table 1. Other sources of RF data have been the Central Radio Propagation Laboratories (CRPL) F-series monthly compilations of solar-geophysical data and reproductions of original records from world-wide sources.

A list of large solar proton events and related phenomena (Table 2) has been compiled from data tabulated by several noted investigators and published in the Goddard Proton Manual.[8] The Goddard data have been checked with other sources of data[1, 12-16] on solar phenomena, and appears to be the most consistent and comprehensive compilation.

In the analysis, possible errors in the data have been taken into consideration. A maximum of a 10% error on the RF emission flux density readings has been taken into account.[17, 18] All time recordings are believed to be correct to plus or minus one minute. The proton event sizes are taken to be correct to a factor of two.

A large solar proton event is defined as having an event size greater than or equal to 10^7 protons/cm^2 at energies greater than

30 Mev. The expression, event size, is used for the integrated omnidirectional particle flux.[8] Thus, a large solar proton event refers to a proton event where the total omnidirectional flux of the particles measured at the earth is greater than 10^7 particles/cm^2 when only those particles of energy greater than 30 Mev are counted.

Associated solar RF emission outbursts have been carefully selected for each large solar proton event. Solar flare data and type IV radio outburst information have been used to aid in the selection of associated solar RF bursts up to 24 hours prior to the start time of the Polar Cap Absorption (PCA) events. (A PCA event is the absorption of galactic radio noise by the ionospheric D-layer over the polar caps. This absorption is produced by an increase in particles from the sun.) The PCA events, solar flare data, and type IV radio outbursts may be found in Table 2. A table has been constructed to show pertinent information related to large solar proton events and their associated RF emission. This table of solar radio emission outbursts, associated with large proton events, may be found in Appendix I.

Records of fixed frequency solar RF bursts from world-wide sources have been reduced and standardized. These solar RF bursts have been studied for signal characteristics indicative of proton events. After studying these records, it becomes evident that each of the RF signals associated with large proton events have several general characteristics in common. (See Figure 1 for an example of a solar radio emission outburst associated with a large proton event.) In particular, the characteristics of signal duration and maximum flux density are related to large proton events. The actual numerical value for the magnitude of these characteristics are different for each frequency. (See Figure 2 for an example of a typical large solar proton event and radio emission relationship.)

In this analysis some specific terms have been defined and are

expressed in their abbreviated form, P(N/A) and P(A/N). P(A/N) is the probability of an alarm being given, provided a proton event of size greater than or equal to a specific event size, N, has occurred. P(N/A) is the probability of a proton event of size equal to or greater than a particular event size occurring, provided an alarm has been given. These conditional probabilities are defined mathematically as follows:

$$P(A/N) = \frac{\Sigma A_i}{\Sigma A_i + \Sigma F_i}$$

$$P(N/A) = 1 - \frac{\Sigma(FA)_i}{\Sigma(FA)_i + \Sigma A_i} = \frac{\Sigma A_i}{\Sigma(FA)_i + \Sigma A_i}$$

$$\text{where, } \Sigma(FA)_i = \Sigma[FA(NPE)]_i + \Sigma[FA(P.E. < N)]_i$$

A_i (an alarm) is a case where the signal, received at a solar radio observatory at a particular frequency, is associated with a prescribed proton event and meets the signal characteristics specified. F_i (an RF failure) is a case where a signal associated with a prescribed proton event does not meet the specified signal characteristics. $(FA)_i$ (a false alarm) is a case where a characteristic signal is received and no proton event (NPE), or a proton event of size less than a specified event size (P.E. < N), is observed.

If a particular case is taken, the P(A/N) basically establishes the following proposition: if a large proton event occurs, then certain characteristics will be met on the RF signal. The P(N/A) establishes the converse proposition to the P(A/N), namely: if certain characteristics are met on the RF signal, then a large proton event will occur.

Two basic approaches have been made in this analysis, a restrictive approach and a non-restrictive approach. In essence, the restrictive approach is overly pessimistic, whereas the non-restrictive approach tends to be optimistic.

In the restrictive approach, the RF failures include cases where a station was in a geographical position to have observed certain RF emissions for a specific solar proton event, but did not report any signal characteristics in the IAU Quarterly Bulletins. Since an observing station did not report any signal characteristics, it has been assumed that the station was in operation at the time of the RF burst but did not receive any signal that met the signal characteristic requirements. The assumption that the observing station did receive a signal but that it did not meet the signal characteristics requirement may not be valid. Examination of original records of solar radio observatories that have been acquired, shows RF bursts for certain proton flares in which signal characteristics were actually met but the RF data simply was not published in the IAU Quarterly. The assumption that the station was actually in operation because it was in a geographical position to have observed the solar RF emissions may be invalid also. The station may have been inoperative for many reasons, such as equipment failure, power failure, etc.

In the non-restrictive approach the proton events included for the analysis were only those that had associated solar RF bursts reported in the IAU Quarterly Bulletins. The results of the non-restrictive analysis are generally higher than the results of the restrictive analysis with respect to the P(A/N).

A statistical analysis has been made on the abstracted IAU data (previously mentioned and found in the appendix) for the determination of optimum frequencies and resultant signal characteristics indicative of large proton events. The optimum frequencies are those with the highest P(A/N) and P(N/A). The initial signal characteristics studied have been signal duration (in minutes) and signal maximum flux density (in 10^{-22} watts M^{-2} $(C/S)^{-1}$).

To determine the optimum frequencies, frequency ranges have been initially selected. Set characteristics have been specified and the

P(A/N) has been determined with respect to these characteristics. This has been done for each of the frequency ranges. (For a list of the frequencies that have been included in each frequency range see the bottom of Table 3.) A 100% P(A/N) refers to a situation in which all RF observations, associated with large proton events, made with frequencies in a particular frequency range met the signal characteristic requirements of duration and maximum flux density. For example, the observatories that are capable (restrictive analysis) of receiving signals between 2000 and 3000 mc/s, have recorded associated bursts which all meet the set signal characteristics (maximum flux density greater than 250 units and signal duration greater than 10 minutes) when the proton event size has been equal to or greater than 10^7 protons/cm^2. at energy greater than 30 Mev.

From the frequency ranges, more reliable [in terms of available data, station handling, and P(A/N)] specific frequencies have been chosen. The analysis then has been continued with respect to these individual frequencies. For each of the individual frequencies the P(A/N), as well as the P(N/A), has been computed with respect to set signal characteristics. For the computation of the P(N/A), the false alarms have also been taken from the IAU Quarterly Bulletins. If a particular projected case is taken, a 25% P(N/A) refers to a situation in which a signal, meeting the characteristic requirements for a large proton event, is received by a solar radio observatory. However, the probability of a large proton event actually accompanying this signal is 25%.

From these studies of individual frequencies, it became obvious that for particular frequencies there is a 100% P(A/N). However, the P(N/A) remains at a rather low level. Since the P(N/A) varies inversely as the false alarms, these phenomena have been studied in an effort to increase the P(N/A) while maintaining a 100% P(A/N). To optimize this situation, additional criteria have been specified on the RF signal characteristics. It has been found that if an increased duration is considered

and the restrictions on maximum flux density are varied for each individual frequency, according to the related proton event size, then the P(N/A) can be increased while the P(A/N) remains at a maximum.

From these studies of maximizing the P(A/N) and P(N/A), the optimum frequencies have been determined. For these optimum frequencies there is a 100% probability of specific RF signal characteristics being met, provided a large proton event of size greater than or equal to a specific event size occurred. Various time studies have been undertaken to determine whether or not these pertinent RF signal characteristics actually precede the start of the PCA event.

These time studies have been made between certain characteristical phases of the associated RF signal and the start of the PCA event as measured at the surface of the earth. Included in this study have been signal duration (SD), rise time to signal maximum flux density (SRT), decay time from signal maximum flux density (SDT), linear rate of rise to maximum flux density (SLRR), delay time between the maximum of the RF signal and start of the PCA event (DMRP), and delay time between the start of the RF signal and start of the PCA event (DSRP). These are defined as follows:

SD = termination time of RF signal - start time of RF signal.

SRT = time of max. of RF signal - start time of RF signal.

SDT = SD - SRT

$$\text{SLRR} = \frac{\text{max. flux density}}{\text{SRT}}$$

DMRP = start time of PCA - time of max. of RF signal.

DSRP = start time of PCA - start time of RF signal.

These time studies have been made on the reliable frequencies, first determined from the frequency range analysis. In these studies, the minimum, maximum, mean, and standard deviation of the time characteristics mentioned have been determined for each frequency.

A further effort has been made to increase the P(N/A) while maintaining a 100% P(A/N). This has been achieved by considering the characteristics of mixed-frequency combinations. Different specific signal characteristics, indicative of large proton events, have been established for each of the three optimum frequencies considered. If these criteria are met on all three frequencies, an associated solar RF burst has been designated an alarm. If no proton event, or a proton event of size less than a specified event size is observed to follow this alarm, then the alarm is a false one. The respective signal durations have been chosen so as to insure sufficient time before the start of the PCA event.

Studies have been made into possible proton event size determinations by using the associated solar RF bursts. In this study, coefficients of rank correlation have been calculated for the relation between proton event size and various characteristics of the associated solar RF signal. The following formula has been used to calculate the respective coefficients-of-rank correlation:[19]

$$r_{rank} = 1 - \frac{6\Sigma D^2}{N(N^2 - 1)}$$

where D = difference between ranks of corresponding values

N = number of pairs of values

The characteristics of the RF signal that have been considered are: those mentioned in the time studies, maximum flux density, and integrated flux density with respect to time. These studies have been made on the optimum frequencies.

The reduced and standardized fixed frequency solar RF bursts have been used for the investigation of the relationship between proton event size and the integrated RF signal flux density with respect to time. In this study the relative areas under the associated solar RF signals have been considered for 10, 20, 30, 40, 50, and 60 minutes after the arrival of the radio outbursts.

STATIONS RECEIVING SOLAR RADIO EMISSION

TABLE 1

Freq. Mc/s	Station	Normal Observing Period Dec. 1961 (Hours U.T.)
9500	Tokyo Astronomical Observatory, Mitaka, Tokyo	00-07
9400	Research Inst. of Atmos. Nagoya Univ., Toyokawa, Japan	23-06
9400	Heinrich Hertz Inst., Berlin-Adlershof	08-14
9100	Netherlands PTT Obser. Station Nera	08-15
3750	Research Inst. of Atmos. Nagoya Univ., Toyokawa, Japan	23-06
3000	Tokyo Astronomical Observatory, Mitaka, Tokyo	00-06
3000	Heinrich Hertz Inst. Berlin-Adlershof	08-14
2980	Netherlands PTT Obser. Station Nera	08-15
2800	National Research Council, Ottawa, Canada	12-21
2000	Research Inst. of Atmos. Nagoya Univ., Toyokawa, Japan	23-06
1500	Heinrich Hertz Inst., Berlin-Adlershof	08-14
1000	Research Inst. of Atmos. Nagoya Univ., Toyokawa, Japan	23-06
808	Astro. Inst. of the Czechoslovak Academy of Sciences, Ondrejov near Prague	08-14
600	Obser. Royal de Belgique, Uccle, Belgium	08-16
545	Netherlands PTT Obser. Station Nera	08-15
545	Surinam Department of Public Works & Traffic & Netherlands PTT Obser. Station Paramaribo	11-21
545	Netherlands PTT Obser. Station Hollandia	21-08
545	Research Inst. of Terrestrial Magnetism, Ionosphere & Radio Propagation, Krasnaia, Pahra, Moscow,	07-12
234	Astroph. Obser. Potsdam, Tremsdorf, Germany	09-14
208	Crimean Astroph. Obser. Crimea, USSR	09-12
208	Ussurijak Radio-Astron. Obser., USSR	21-01
208	Research Inst. of Terrestrial Magnetism Ionosphere & Radio Propagation, Krasnaia, Pahra, Moscow	07-12
200	Hiraiso Radio Wave Obser., Japan	23-08
200	Tokyo Astronomical Observatory, Mitaka, Japan	00-06
200	Netherlands PTT Obser. Station Nera	08-15
200	Surinam Department of Public Works & Traffic & Netherlands PTT Obser. Station Paramaribo	11-21
200	Netherlands PTT Obser. Station Hollandia	21-08
178	Kislovodsk Radio-Astronomical Obser., USSR	07-12
169	Obser. de Paris, Meudon, Nancay Station	11-13
127	Astronomical Obser. of the New Copernicus Univ., Poland	09-15
111	Astroph. Obser. Potsdam, Tremsdorf, Germany	09-14
108	National Bureau of Standards, Central Radio Propagation Lab. Boulder, USA	14-23
100	Tokyo Astronomical Observatory, Mitaka, Tokyo	00-06
23	Astroph. Obser. Potsdam, Tremsdorf, Germany	09-14
18	National Bureau of Standards, Central Radio Propagation Lab. Boulder, USA	14-23

LARGE SOLAR PROTON EVENTS AND RELATED PHENOMENA

TABLE 2

Date	Solar Flare Time of Max. (U.T.)	Start Time of Type-IV Radio Outburst (U.T.)	Proton Event Size (E > 30 Mev)	Date	PCA Event Start Time (U.T.)
2-23-56	0342	0330	1.6×10^9	2-23-56	0430
8-31-56	1241	1231	3×10^7	8-31-56	1500
1-20-57	1120	1255	3×10^8	1-20-57	1500
7-3-57	0740	0832	10^7	7-3-57	0845
8-31-57	1312	1302	10^7	8-31-57	1530
10-20-57	1642	1636	10^7	10-21-57	0630
3-23-58	1005	1003	4×10^8	3-23-58	1830
7-7-58	0033	0026	5×10^8	7-7-58	0130
8-16-58	0440	0448	2×10^7	8-16-58	0600
8-22-58	1448	1430	5×10^7	8-22-58	1530
8-26-58	0027	0023	5.3×10^7	8-26-58	0100
5-10-59	2140	2100	1.2×10^9	5-10-59	2300
7-10-59	0240	0223	8×10^8	7-10-59	0400
7-14-59	0349	0330	2×10^9	7-14-59	0700
7-16-59	2132	2118	3×10^9	7-17-59	0200
4-28-60	0137	0145	2.5×10^7	4-28-60	0200
9-3-60	0037	0035	4×10^7	9-3-60	0800
11-12-60	1330	1327	2.7×10^9	11-12-60	1445
11-15-60	0221	0221	2×10^9	11-15-60	0505
11-20-60	2020	2023	6×10^7	11-21-60	0500
7-12-61	1025	1025	10^7	7-13-61	0700
7-18-61	1000	0940	2.5×10^8	7-18-61	1135
9-28-61	2223	2212	10^7	9-28-61	2335

FIG. 1

EXAMPLE OF RF EMISSION ASSOCIATED WITH PROTON EVENT

FEBRUARY 23, 1956

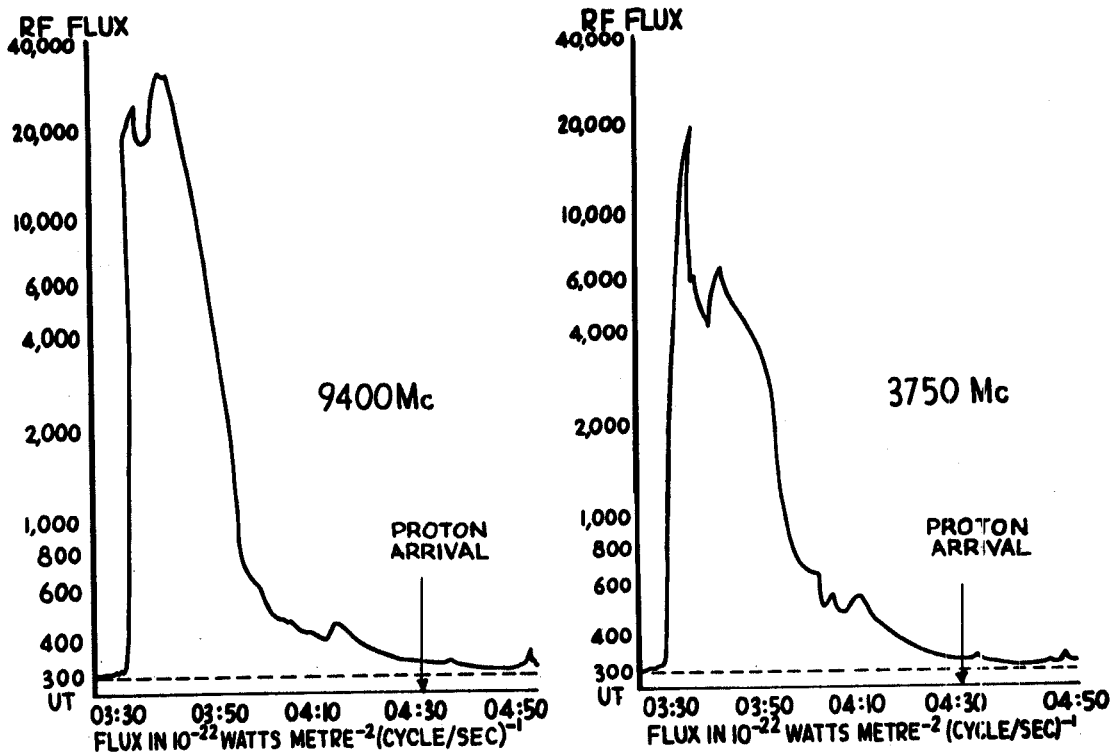

FIG. 2

TYPICAL PROTON EVENT & RF EMISSION RELATIONSHIP

AUG 22, 1958 – 5×10^7 PROTONS/CM^2

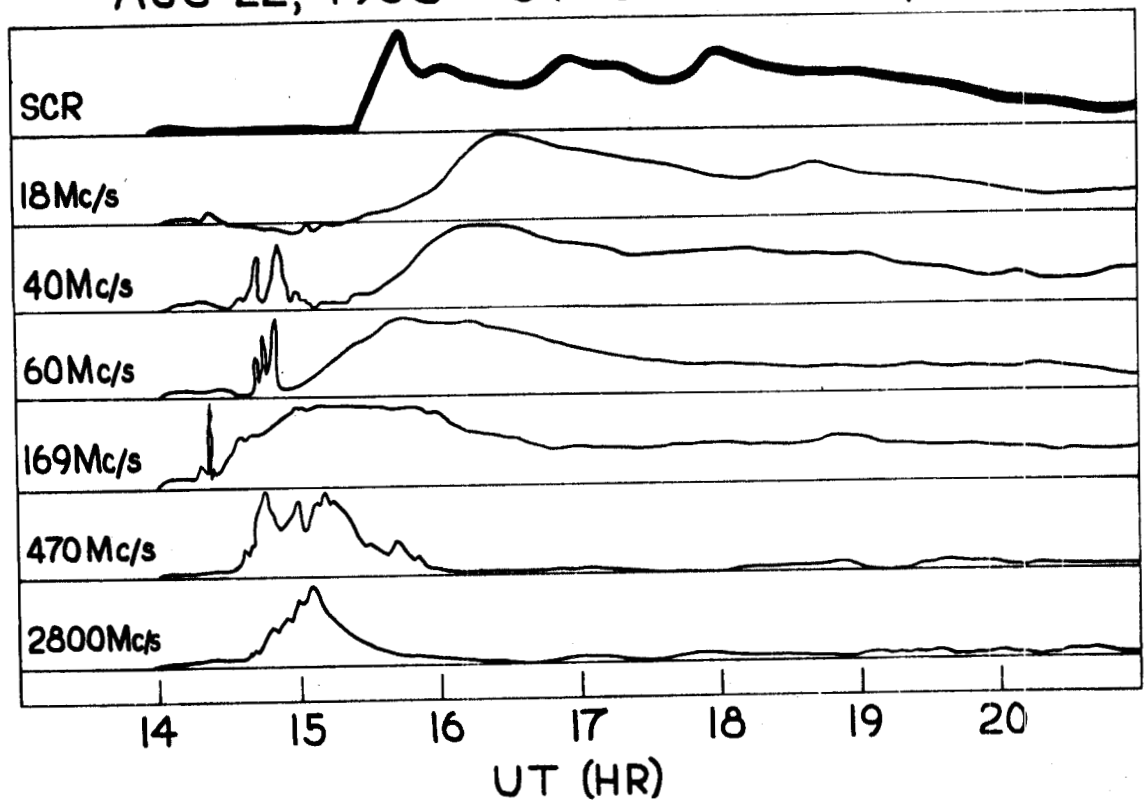

RESULTS

The P(A/N) for various frequency ranges may be found in Tables 3 and 4. The P(A/N) has been calculated with respect to the proton event size and the signal characteristics specified in the tables. Table 3 is for the restrictive approach while Table 4 is for the non-restrictive approach. For a graphical comparison between the frequency ranges with respect to the P(A/N) see Figure 3.

The results obtained from studying the reliable individual frequencies are shown in Tables 5-8. These results are presented in a similar manner as those obtained for the frequency ranges. The P(N/A), an additional computation, is shown in the last column of the individual frequency tables. For a graphical comparison between the individual frequencies with respect to the P(A/N) and P(N/A) see Figure 4.

As mentioned previously, the optimum frequencies are those with the highest P(A/N) and P(N/A). From Figures 3 and 4 the optimum frequencies appear to lie in the range of 1000 - 3750 mc/s. In particular, 1000, 2000, 2800, and 3750 mc/s appear to be the optimum frequencies.

The results of the studies to maximize the P(A/N) and P(N/A) on the optimum frequencies may be shown graphically in Figure 5. These frequencies are considered with a signal duration greater than 25 minutes and a varied maximum flux density. With these signal conditions on 3750 mc/s and the proton event size equal to or greater than 10^7 protons/cm^2, the P(A/N) is 100% while the P(N/A) is 33%.

Tables 9 and 10 contain the results of the time studies. For associated solar RF signal SD, SRT, SDT, and DMRP for large proton events see Table 9. The DSRP for proton events of size greater than or equal to 10^7, 10^8, and 10^9 protons/cm^2, respectively, may be found in Table 10.

For a graph of the delay times between the start of the RF signal and start of the PCA event (DSRP), for the optimum frequencies, with respect to proton event sizes equal to or greater than 10^7, 10^8, and 10^9 protons/cm^2, respectively see Figure 6. It should be noted that as the proton event size increases, the maximum DSRP decreases and the minimum increases. The shortest DSRP for large proton events and frequencies in the range from 200-9400 mc/s is 25 minutes. This gives sufficient time to recognize an alarm on a solar RF burst. The mean DSRP is 178 minutes with a maximum of 826 minutes. From the standard deviations from the mean DSRP, for each of the frequencies (Table 10), it can be seen that there is a strong tendency toward the occurrence of the shorter DSRP.

The signal characteristics of duration and maximum flux density, specified in this study for the indication of large proton events, can be detected on the optimum frequencies prior to the start of the PCA event in every case. To support this statement the following observations have been made from Tables 9 and 10:

1. The signal is of sufficient duration to give an alarm in every case.
2. The signal maximum occurs early in the lifetime of the burst.
3. The signal maximum occurs before the start of the PCA event in every case.
4. The minimum delay times, between the start of the RF signal and the start of the PCA event, are equal to or greater than the duration necessary to give an alarm in every case.

The consideration of mixed frequency combinations show that the P(N/A) can be increased while maintaining a 100% P(A/N). The frequencies used are the previously determined optimum frequencies of 1000, 2000, and 3750 mc/s. In Table 11 the pertinent information for the calculation of the P(A/N) and P(N/A) is listed in addition to the results. These results are for both restrictive and non-restrictive approaches. With the signal characteristics specified, on each of the

three frequencies, the P(A/N) is 100% while the P(N/A) is 57% for large proton events.

The P(N/A) can thus be increased, while maintaining a 100% P(A/N), by consideration of more specific signal characteristics and mixed frequency combinations. For a graph comparing the reduction of the P(N/A) by different means, see Figure 7. By consideration of additional methods, it has been found that the P(N/A) cannot be appreciably increased beyond 57% without lowering the 100% P(A/N). This leads to the conclusion that the false alarms are a permanent phenomena and some additional means are necessary to explain them.

Studies into possible proton event size determinations have shown that the size of a proton event cannot be determined with complete accuracy by using the associated solar RF bursts. (See Table 12 for the basic results of these studies.) There is, however, an indication of a relationship. This relationship is evident when the RF signal integrated flux density with respect to time is compared with the proton event size. The rank correlation coefficients expressing this relationship, for each of the times considered, on the frequencies of 1000, 2000, and 3750 mc/s are shown in Figures 8-10. It should be noted that the rank correlation coefficient is 0.83 for the relationship between the proton event size and the area under the associated signal after 20 minutes have elapsed after the arrival of the burst on 2000 mc/s.

FREQUENCY RANGES
(RESTRICTIVE APPROACH)

TABLE 3

Proton Event Size (N) in Protons/cm^2 with E > 30 Mev	Associated Solar Radio Outbursts: Frequency Range Mc/s	Duration (min.)	Max. Flux Density Inst. or Smooth 10^{-22} wm^{-2} (C/S)$^{-1}$	P(A/N) (%)
$\geq 10^7$	<450	>10	>200	89%
$\geq 10^8$	<450	>10	>200	90%
$\geq 10^9$	<450	>10	>200	100%
$\geq 10^8$	450-808	>10	>250	100%
$\geq 10^7$	450-808	>10	>250	76%
$\geq 10^7$	450-808	>10	>150	83%
$\geq 10^7$	810-1500	>10	>250	94%
$\geq 10^8$	810-1500	>20	>250	100%
$\geq 10^7$	810-1500	>20	>350	81%
$\geq 10^8$	810-1500	>20	>350	100%
$\geq 10^7$	1420-2000	>10	>200	81%
$\geq 10^8$	1420-2000	>10	>200	87%
$\geq 10^9$	1420-2000	>10	>200	100%
$\geq 10^7$	2000-3000	>10	>250	100%
$\geq 10^7$	2000-3000	>20	>250	95%
$\geq 10^8$	2000-3000	>20	>250	100%
$\geq 10^7$	2800-3750	>10	>150	100%
$\geq 10^7$	2800-3750	>20	>350	90%
$\geq 10^8$	2800-3750	>20	>350	91%
$\geq 10^9$	2800-3750	>20	>350	100%
$\geq 10^7$	>3750	>10	>250	88%
$\geq 10^8$	>3750	>10	>250	86%
$\geq 10^9$	>3750	>10	>250	100%

Frequency Range (Mc/s)	Included Frequencies
<450	231,209,207,203,201,200,178,169,167,108,81,80,23,18,
450-808	450,536,538,545,600,808
810-1500	810,1000,1420,1500
1420-2000	1420,1500,2000
2000-3000	2000,2800,2980,3000
2800-3750	2800,2980,3000,3750
>3750	9100,9375,9400,9500

FREQUENCY RANGES
(NON-RESTRICTIVE APPROACH)

TABLE 4

Proton Event Size (N) in Protons/cm^2 with E > 30 Mev	Associated Solar Radio Outbursts			
	Frequency Range Mc/s	Duration (min.)	Max. Flux Density Inst. or Smooth 10^{-22} wm-2 (C/S)$^{-1}$	P(A/N) (%)
$\geq 10^7$	<450	>10	>300	100%
$\geq 10^7$	<450	>25	>500	94%
$\geq 10^8$	<450	>25	>500	100%
$\geq 10^7$	450-808	>10	>150	83%
$\geq 10^8$	450-808	>10	>150	100%
$\geq 10^7$	810-1500	>20	>250	100%
$\geq 10^7$	810-1500	>25	>600	80%
$\geq 10^8$	810-1500	>25	>600	100%
$\geq 10^7$	1420-2000	>25	>150	100%
$\geq 10^7$	1420-2000	>25	>750	72%
$\geq 10^8$	1420-2000	>25	>750	100%
$\geq 10^7$	1420-2800	>25	>150	100%
$\geq 10^7$	1420-2800	>25	>750	88%
$\geq 10^8$	1420-2800	>25	>750	100%
$\geq 10^7$	2000-3000	>25	>750	85%
$\geq 10^8$	2000-3000	>25	>750	100%
$\geq 10^7$	2000-3000	>10	>250	100%
$\geq 10^7$	2800-3750	>10	>150	100%
$\geq 10^7$	>3750	>25	>250	100%
$\geq 10^7$	>3750	>25	>1250	79%
$\geq 10^8$	>3750	>25	>1250	100%

FIG. 3

FREQUENCY RANGES

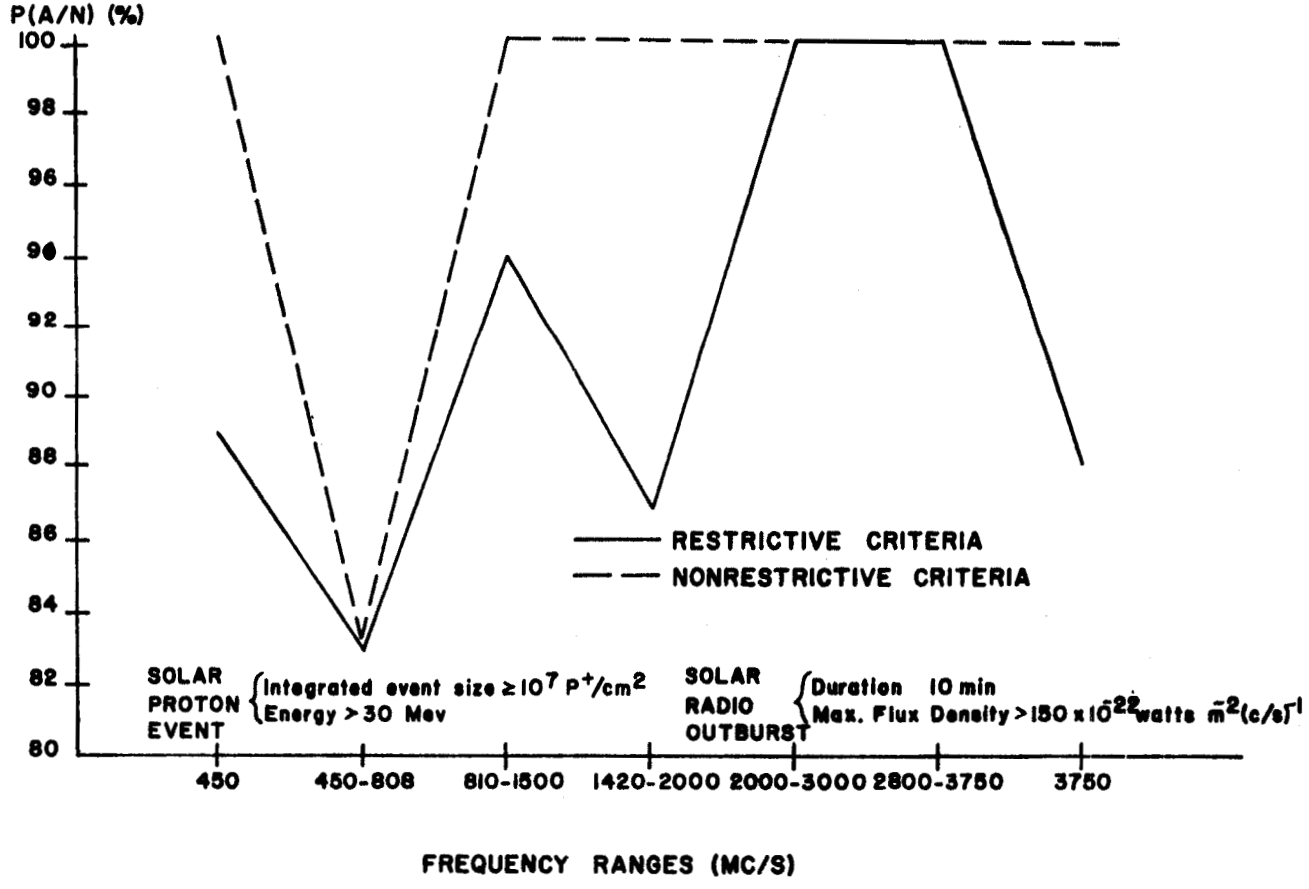

INDIVIDUAL FREQUENCIES

(RESTRICTIVE APPROACH)

TABLE 5

Proton Event Size (N) in Protons/cm^2 with E > 30 Mev	Associated Solar Radio Outburst			P(A/N) (%)	P(N/A) (%)
	Frequency (Mc/s)	Duration (min.)	Max. Flux Density Inst. or Smooth 10^{-22} wm^{-2} (C/S)$^{-1}$		
$\geq 10^7$	200	>10	>150	71%	7%
$\geq 10^8$	200	>10	>150	75%	4%
$\geq 10^9$	200	>10	>150	100%	3%
$\geq 10^7$	545	>10	>150	75%	10%
$\geq 10^8$	545	>10	>150	90%	7%
$\geq 10^9$	545	>10	>150	100%	4%
$\geq 10^7$	545	>25	>350	60%	19%
$\geq 10^8$	545	>25	>350	90%	14%
$\geq 10^9$	545	>25	>350	100%	9%
$\geq 10^7$	1000	>10	>150	100%	13%
$\geq 10^8$	1000	>10	>150	100%	7%
$\geq 10^9$	1000	>10	>150	100%	5%
$\geq 10^7$	1000	>25	>250	100%	25%
$\geq 10^8$	1000	>25	>250	100%	10%
$\geq 10^9$	1000	>25	>250	100%	10%
$\geq 10^7$	1000	>25	>800	83%	37%
$\geq 10^8$	1000	>25	>800	100%	24%
$\geq 10^9$	1000	>25	>800	100%	17%
$\geq 10^9$	1000	>25	>1600	100%	25%
$\geq 10^7$	1420	>10	>150	31%	12%
$\geq 10^8$	1420	>10	>150	40%	6%
$\geq 10^9$	1420	>10	>150	100%	3%
$\geq 10^7$	2000	>10	>150	100%	20%
$\geq 10^8$	2000	>10	>150	100%	11%
$\geq 10^9$	2000	>10	>150	100%	6%
$\geq 10^7$	2000	>25	>150	100%	32%
$\geq 10^8$	2000	>25	>150	100%	17%
$\geq 10^9$	2000	>25	>150	100%	10%
$\geq 10^7$	2000	>25	>1000	85%	58%
$\geq 10^8$	2000	>25	>1000	100%	37%
$\geq 10^9$	2000	>25	>1000	100%	21%
$\geq 10^7$	2000	>25	>1300	77%	67%
$\geq 10^8$	2000	>25	>1300	86%	40%
$\geq 10^9$	2000	>25	>1300	100%	27%

INDIVIDUAL FREQUENCIES

(RESTRICTIVE APPROACH)

TABLE 6

Proton Event Size (N) in Protons/cm^2 with E>30 Mev	Frequency (Mc/s)	Duration (min.)	Max. Flux Density Inst. or Smooth 10^{-22} wm^{-2} (C/S)$^{-1}$	P(A/N) (%)	P(N/A) (%)
$\geq 10^7$	2800	>10	>150	100%	5%
$\geq 10^8$	2800	>10	>150	100%	3%
$\geq 10^9$	2800	>10	>150	100%	2%
$\geq 10^7$	2800	>25	>400	100%	18%
$\geq 10^8$	2800	>25	>400	100%	9%
$\geq 10^9$	2800	>25	>400	100%	7%
$\geq 10^7$	2800	>25	>800	62%	19%
$\geq 10^8$	2800	>25	>800	100%	15%
$\geq 10^9$	2800	>25	>2500	100%	75%
$\geq 10^7$	3750	>10	>150	100%	16%
$\geq 10^8$	3750	>10	>150	100%	7%
$\geq 10^9$	3750	>10	150	100%	5%
$\geq 10^7$	3750	>25	>250	100%	33%
$\geq 10^8$	3750	>25	>250	100%	15%
$\geq 10^9$	3750	>25	>250	100%	10%
$\geq 10^7$	3750	>25	>1500	77%	53%
$\geq 10^8$	3750	>25	>1500	100%	32%
$\geq 10^9$	3750	>25	>1500	100%	21%
$\geq 10^7$	9400	>10	>150	68%	3%
$\geq 10^8$	9400	>10	>150	78%	2%
$\geq 10^9$	9400	>10	>150	100%	1%

INDIVIDUAL FREQUENCIES

(NON-RESTRICTIVE APPROACH)

TABLE 7

Proton Event Size (N) in Protons/cm^2 with E > 30 Mev	Associated Solar Radio Outburst			P(A/N) (%)	P(N/A) (%)
	Frequency (Mc/s)	Duration (min.)	Max. Flux Density Inst. or Smooth 10^{-22} wm^{-2} (C/S)$^{-1}$		
$\geq 10^7$	200	>10	>150	83%	7%
$\geq 10^8$	200	>10	>150	100%	4%
$\geq 10^9$	200	>10	>150	100%	3%
$\geq 10^7$	200	>20	>350	83%	10%
$\geq 10^8$	200	>20	>350	100%	6%
$\geq 10^9$	200	>20	>350	100%	4%
$\geq 10^7$	545	>10	>150	94%	10%
$\geq 10^8$	545	>10	>150	100%	7%
$\geq 10^9$	545	>10	>150	100%	4%
$\geq 10^7$	545	>25	>350	80%	19%
$\geq 10^8$	545	>25	>350	100%	14%
$\geq 10^9$	545	>25	>350	100%	9%
$\geq 10^7$	1000	>10	>150	100%	13%
$\geq 10^8$	1000	>10	>150	100%	7%
$\geq 10^9$	1000	>10	>150	100%	5%
$\geq 10^7$	1000	>25	>250	100%	25%
$\geq 10^8$	1000	>25	>250	100%	10%
$\geq 10^9$	1000	>25	>250	100%	10%
$\geq 10^7$	1000	>25	>800	83%	37%
$\geq 10^8$	1000	>25	>800	100%	24%
$\geq 10^9$	1000	>25	>800	100%	17%
$\geq 10^9$	1000	>25	>1600	100%	25%
$\geq 10^7$	1420	>10	>150	100%	12%
$\geq 10^8$	1420	>10	>150	100%	6%
$\geq 10^9$	1420	>10	>150	100%	3%
$\geq 10^7$	1420	>25	>150	100%	25%
$\geq 10^8$	1420	>25	>150	100%	13%
$\geq 10^9$	1420	>25	>150	100%	6%
$\geq 10^7$	2000	>10	>150	100%	20%
$\geq 10^8$	2000	>10	>150	100%	11%
$\geq 10^9$	2000	>10	>150	100%	6%
$\geq 10^7$	2000	>25	>150	100%	32%
$\geq 10^8$	2000	>25	>150	100%	17%
$\geq 10^9$	2000	>25	>150	100%	10%

INDIVIDUAL FREQUENCIES
(NON-RESTRICTIVE APPROACH)

TABLE 8

Proton Event Size (N) in Protons/cm^2 with E > 30 Mev	Associated Solar Radio Outbursts			P(A/N) (%)	P(N/A) (%)
	Frequency (Mc/s)	Duration (min.)	Max. Flux Density Inst. or Smooth 10^{-22} wm^{-2} (C/S)$^{-1}$		
$\geq 10^7$	2000	>25	>1000	85%	58%
$\geq 10^8$	2000	>25	>1000	100%	37%
$\geq 10^9$	2000	>25	>1000	100%	21%
$\geq 10^7$	2000	>25	>1300	77%	67%
$\geq 10^8$	2000	>25	>1300	86%	40%
$\geq 10^9$	2000	>25	>1300	100%	27%
$\geq 10^7$	2800	>10	>150	100%	5%
$\geq 10^8$	2800	>10	>150	100%	3%
$\geq 10^9$	2800	>10	>150	100%	2%
$\geq 10^7$	2800	>25	>400	100%	19%
$\geq 10^8$	2800	>25	>400	100%	9%
$\geq 10^9$	2800	>25	>400	100%	7%
$\geq 10^7$	2800	>25	>800	62%	19%
$\geq 10^8$	2800	>25	>800	100%	15%
$\geq 10^9$	2800	>25	>2500	100%	75%
$\geq 10^7$	3750	>10	>150	100%	16%
$\geq 10^8$	3750	>10	>150	100%	7%
$\geq 10^9$	3750	>10	>150	100%	5%
$\geq 10^7$	3750	>25	>250	100%	33%
$\geq 10^8$	3750	>25	>250	100%	15%
$\geq 10^9$	3750	>25	>250	100%	10%
$\geq 10^7$	3750	>25	>1500	77%	53%
$\geq 10^8$	3750	>25	>1500	100%	32%
$\geq 10^9$	3750	>25	>1500	100%	21%
$\geq 10^7$	9400	>10	>150	100%	3%
$\geq 10^8$	9400	>10	>150	100%	2%
$\geq 10^9$	9400	>10	>150	100%	1%
$\geq 10^7$	9400	>20	>150	100%	6%
$\geq 10^8$	9400	>20	>150	100%	3%
$\geq 10^9$	9400	>20	>150	100%	2%
$\geq 10^7$	9400	>25	>600	85%	19%
$\geq 10^8$	9400	>25	>600	100%	12%
$\geq 10^9$	9400	>25	>600	100%	8%

FIG. 4

RELIABLE FREQUENCIES

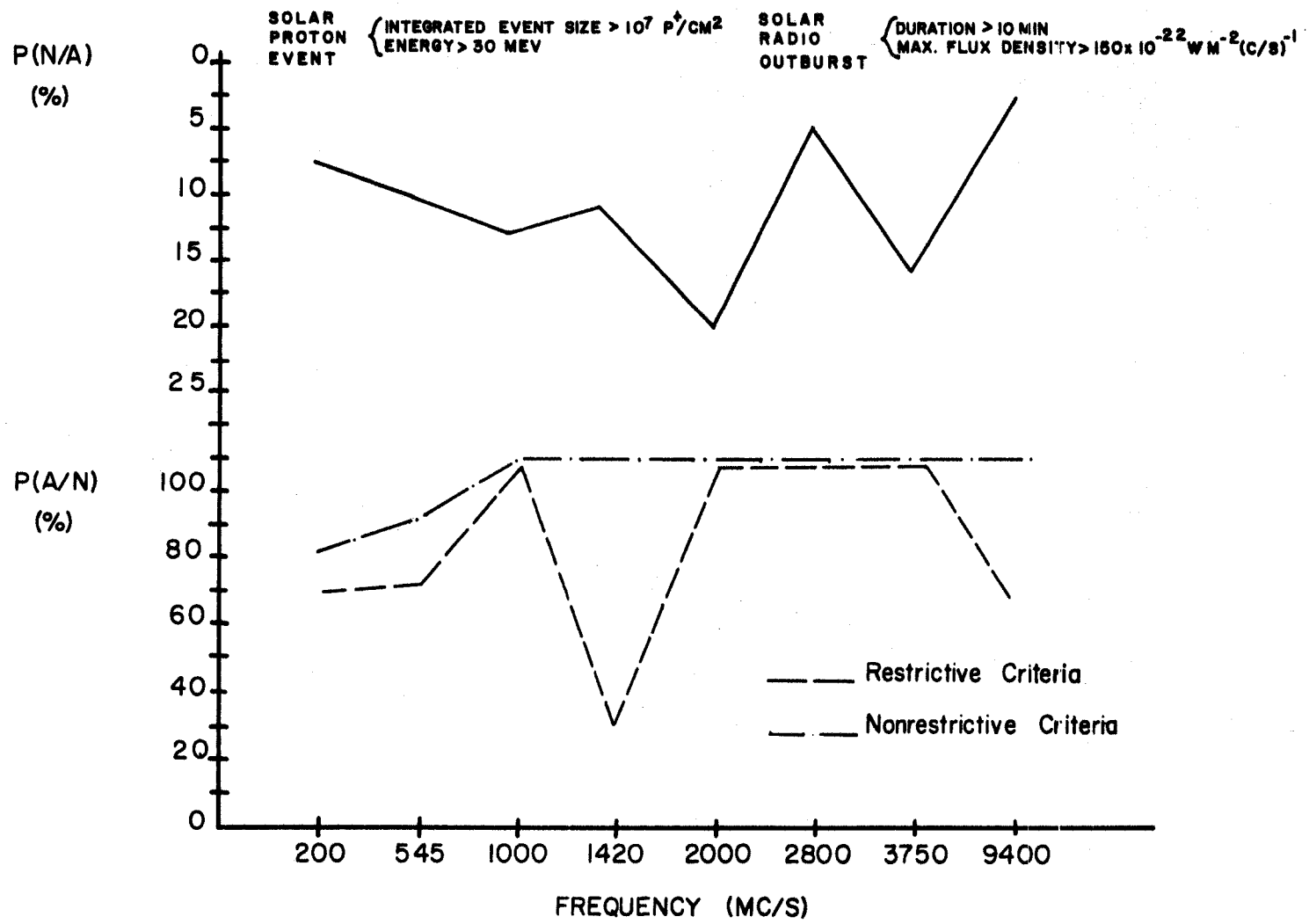

FIG. 5

OPTIMUM FREQUENCIES P(A/N) = 100%

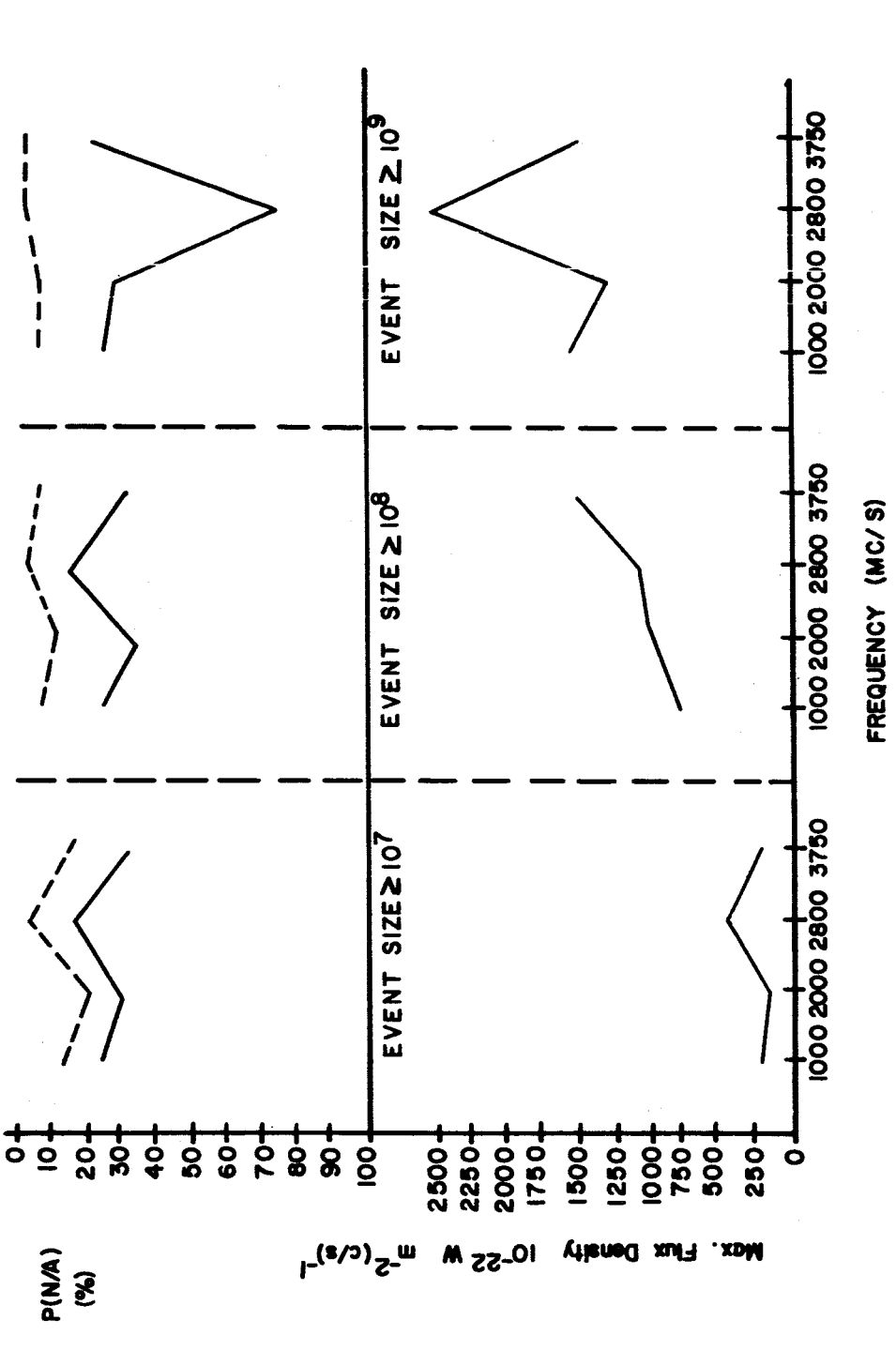

CHARACTERISTICS OF ASSOCIATED RF BURSTS FOR LARGE PROTON EVENTS
(PE SIZE $\geq 10^7$ PT/CM^2)

TABLE 9

SIGNAL CHARACTERISTIC	FREQUENCY MC/S	MAXIMUM	MINIMUM	MEAN	STANDARD DEVIATION
SIGNAL DURATION (minutes)	200	600	5	145	151
	545	165	5	82	54
	1000	235	45	74	37
	1420	131	17	82	48
	2000	125	30	72	38
	2800	340	30	120	107
	3750	100	30	57	21
	9400	172	30	70	44
RISE TIME TO SIGNAL MAX. FLUX DENSITY (minutes)	200	35	1	21	15
	1000	51	1	20	18
	1420	32	4	21	15
	2000	49	2	21	17
	2800	49	1	21	18
	3750	36	1	13	11
	9400	72	1	20	22
DECAY TIME FROM SIGNAL MAX. FLUX DENSITY (minutes)	200	119	12	66	55
	1000	230	13	70	59
	1420	63	13	45	28
	2000	87	7	50	28
	2800	315	23	99	97
	3750	260	14	64	66
	9400	144	21	53	36
DELAY TIME BETWEEN THE MAX. OF THE RF SIGNAL & START OF THE PCA EVENT (minutes)	200	555	59	187	245
	1000	589	18	151	197
	1420	80	17	38	36
	2000	580	18	152	182
	2800	819	24	234	287
	3750	415	19	144	162
	9400	581	3	176	196

DELAY BETWEEN START OF THE RF SIGNAL AND START OF THE PCA EVENT
(MINUTES)

TABLE 10

Proton Event Size (pt/cm^2)	Frequency Mc/s	Maximum	Minimum	Mean	Standard Deviation
$\geq 10^7$	200	590	41	183	178
$\geq 10^7$	545	582	25	205	194
$\geq 10^7$	1000	590	29	164	187
$\geq 10^7$	1420	210	44	97	78
$\geq 10^7$	2000	582	35	169	182
$\geq 10^7$	2800	826	60	255	279
$\geq 10^7$	3750	522	28	157	161
$\geq 10^7$	9400	582	27	197	190
$\geq 10^8$	200	280	55	132	79
$\geq 10^8$	545	507	63	205	152
$\geq 10^8$	1000	209	29	128	77
$\geq 10^8$	1420	210	49	130	114
$\geq 10^8$	2000	209	35	130	75
$\geq 10^8$	2800	282	64	138	99
$\geq 10^8$	3750	210	28	114	76
$\geq 10^8$	9400	210	27	130	79
$\geq 10^9$	200	280	55	135	66
$\geq 10^9$	545	286	79	170	93
$\geq 10^9$	1000	209	163	186	33
$\geq 10^9$	2000	209	165	187	31
$\geq 10^9$	2800	282	85	162	105
$\geq 10^9$	3750	210	56	144	79
$\geq 10^9$	9400	210	118	165	46

FIG. 6

RF START DELAY TIMES VS FREQUENCY

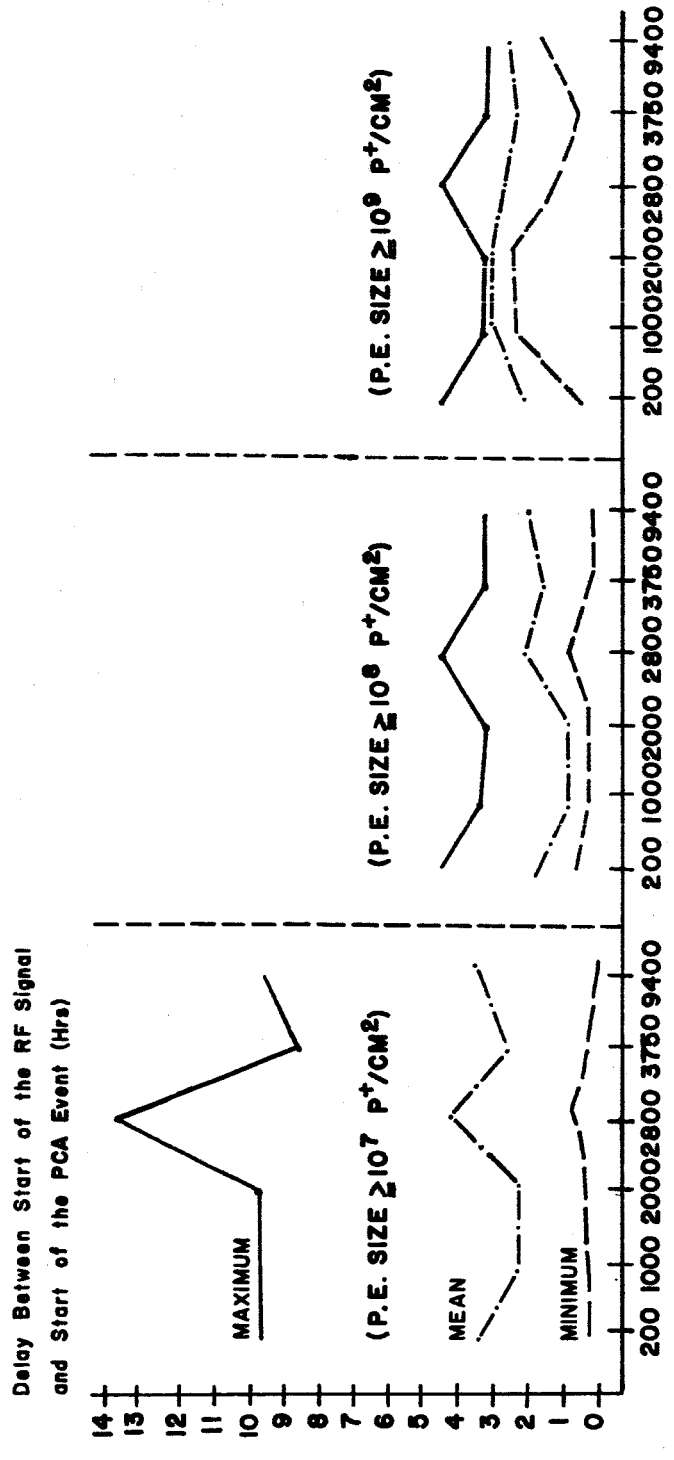

MIXED FREQUENCIES

TABLE II

Proton Event Size (Pt/cm^2)	1000 mc/s		2000 mc/s		3750 mc/s		$\sum A_i$	$\sum F_i$	P(A/N) (%)	$\sum (FA)_i$ P.E.>N	$\sum (FA)_i$ (NPE)	$\sum (FA)_i$	P(N/A) (%)
	Dura.	M.F.D.	Dura.	M.F.D.	Dura.	M.F.D							
$>10^7$	>25	> 250	>25	>150	>25	> 250	13	0	100%	5	5	10	57%
$>10^8$	>25	> 800	>25	>1000	>25	>1500	6	4	100%	6	1	7	46%
$>10^9$	>80	>1500	>80	>1300	>50	>1500	4	0	100%	5	0	5	56%

FIG. 7

P(N/A) WITH P(A/N) = 100%

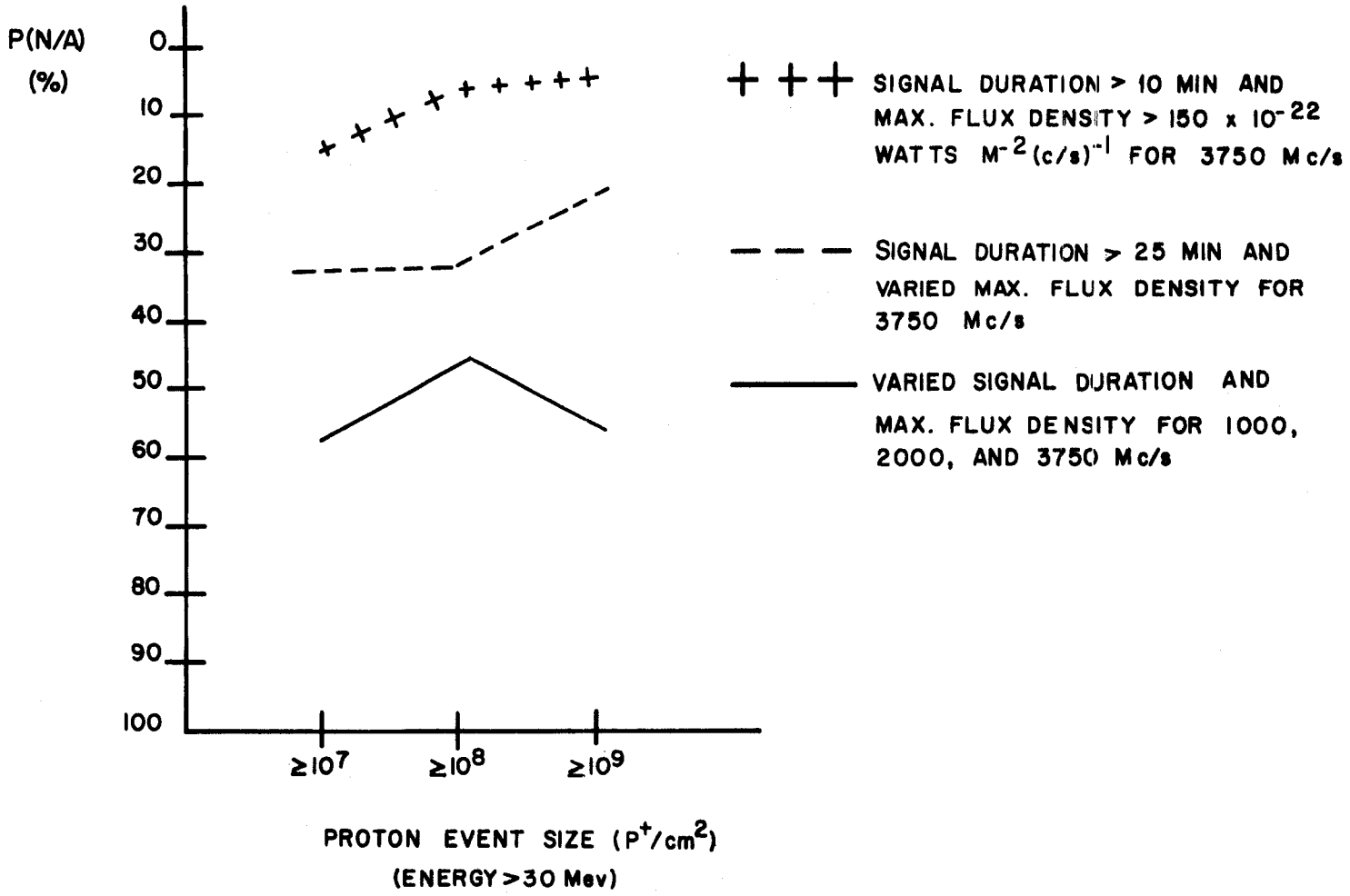

SOLAR RADIO OUTBURSTS AND PROTON EVENT SIZE

TABLE 12

Frequency	Signal Characteristic	Coefficient of Rank Correlation Between Proton Event Size and the Associated Solar RF Signal Characteristic Specified
1000	Duration	0.66
1000	Maximum Flux Density (MFD)	0.47
1000	Rise Time to Sig. MFD	0.22
1000	Linear Rate of Rise to MFD	0.40
1000	Decay Time from MFD	0.17
1000	Start Delay Time	0.52
1000	Signal Max. Delay Time	0.31
2000	Duration	0.60
2000	Maximum Flux Density (MFD)	0.56
2000	Rise Time to Sig. MFD	0.28
2000	Linear Rate of Rise to MFD	0.40
2000	Decay Time from MFD	0.41
2000	Start Delay Time	0.09
2000	Signal Max. Delay Time	0.09
2800	Duration	0.69
2800	Maximum Flux Density (MFD)	0.58
2800	Rise Time to Sig. MFD	0.57
2800	Linear Rate of Rise to MFD	0.12
2800	Decay Time from MFD	0.73
2800	Start Delay Time	0.04
2800	Signal Max. Delay Time	0.00
3750	Duration	0.31
3750	Maximum Flux Density (MFD)	0.49
3750	Rise Time to Sig. MFD	0.17
3750	Linear Rate of Rise to MFD	0.54
3750	Decay Time from MFD	0.20
3750	Start Delay Time	0.03
3750	Signal Max. Delay Time	0.01

FIG. 8

AREA UNDER RF OUTBURST & PROTON EVENT SIZE

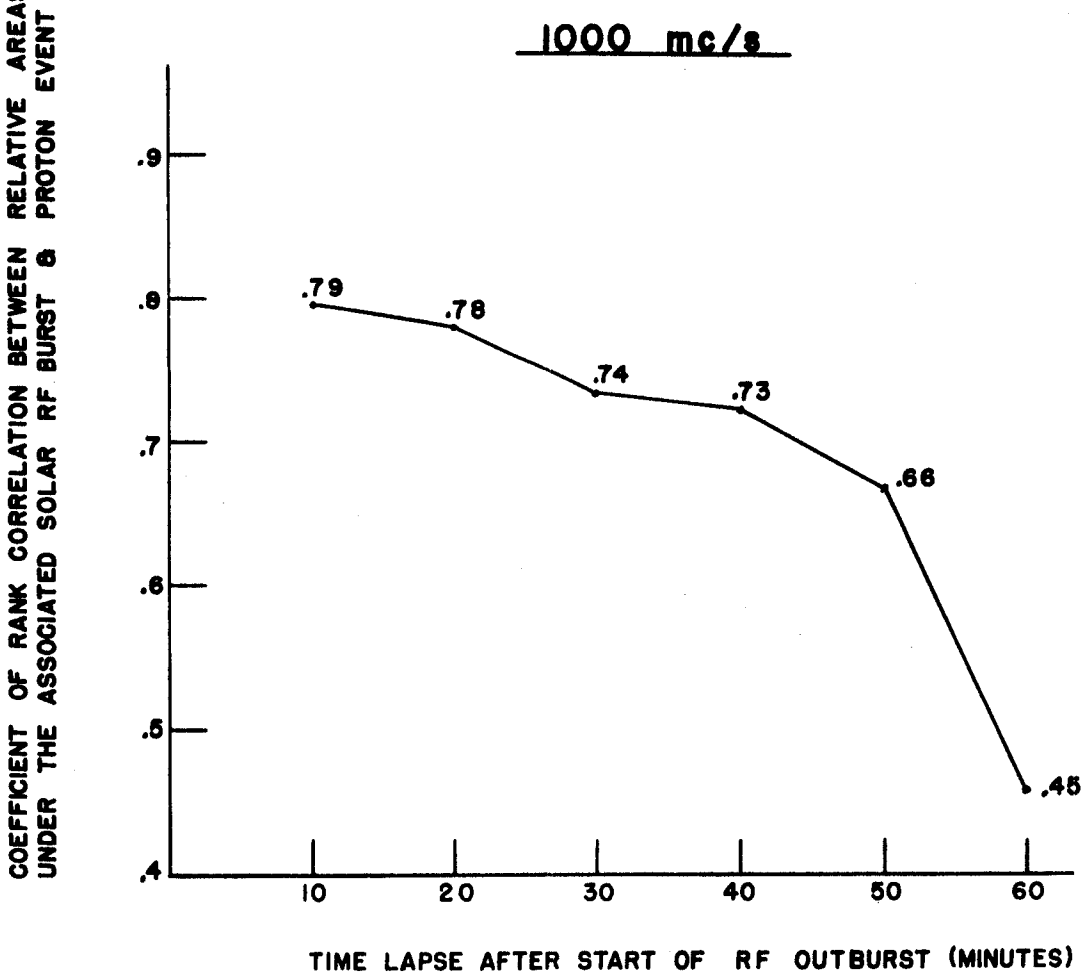

FIG. 9

RF AREA AND SOLAR PROTON EVENT SIZE

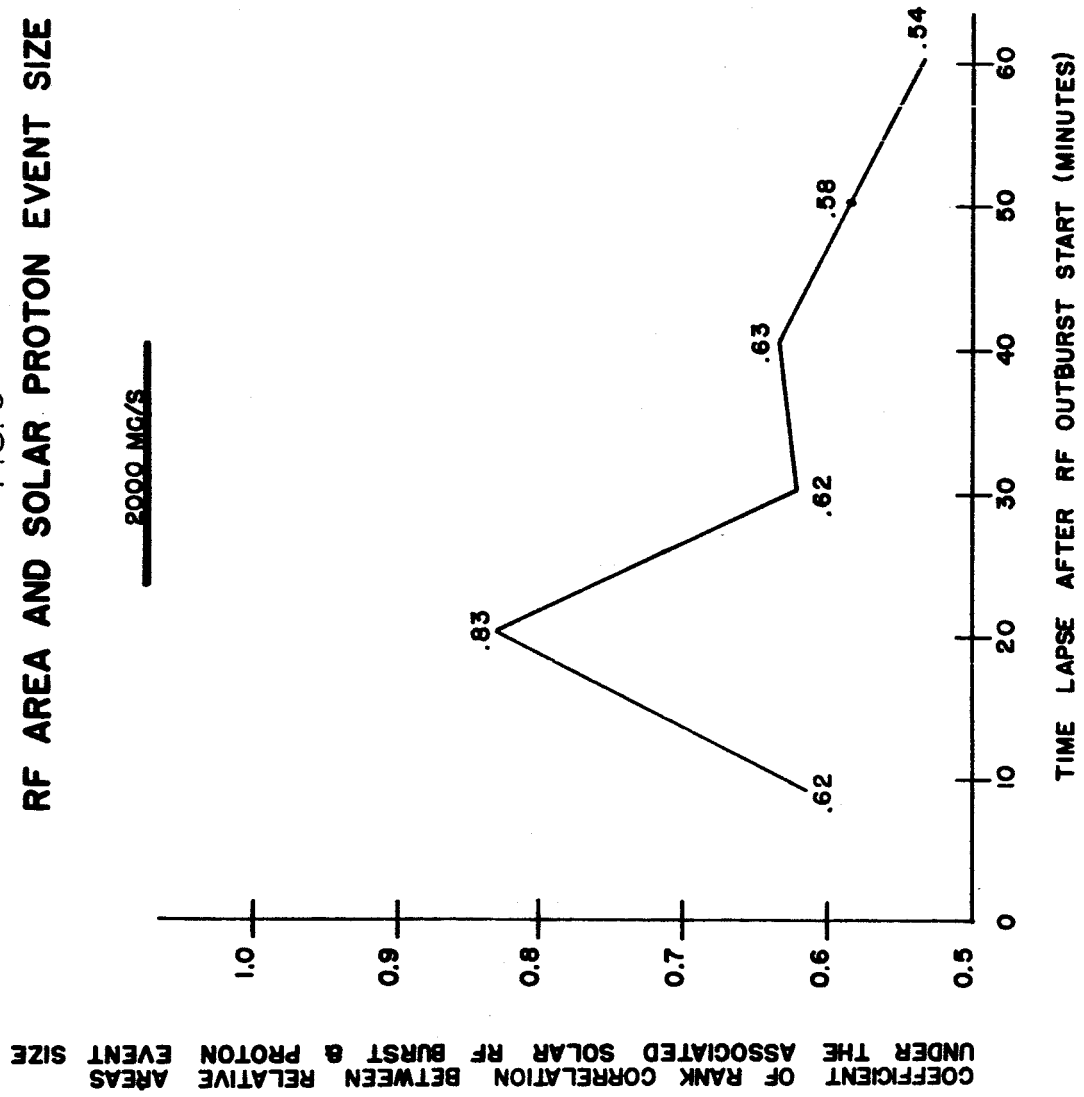

FIG. 10

AREA UNDER RF OUTBURST & PROTON EVENT SIZE

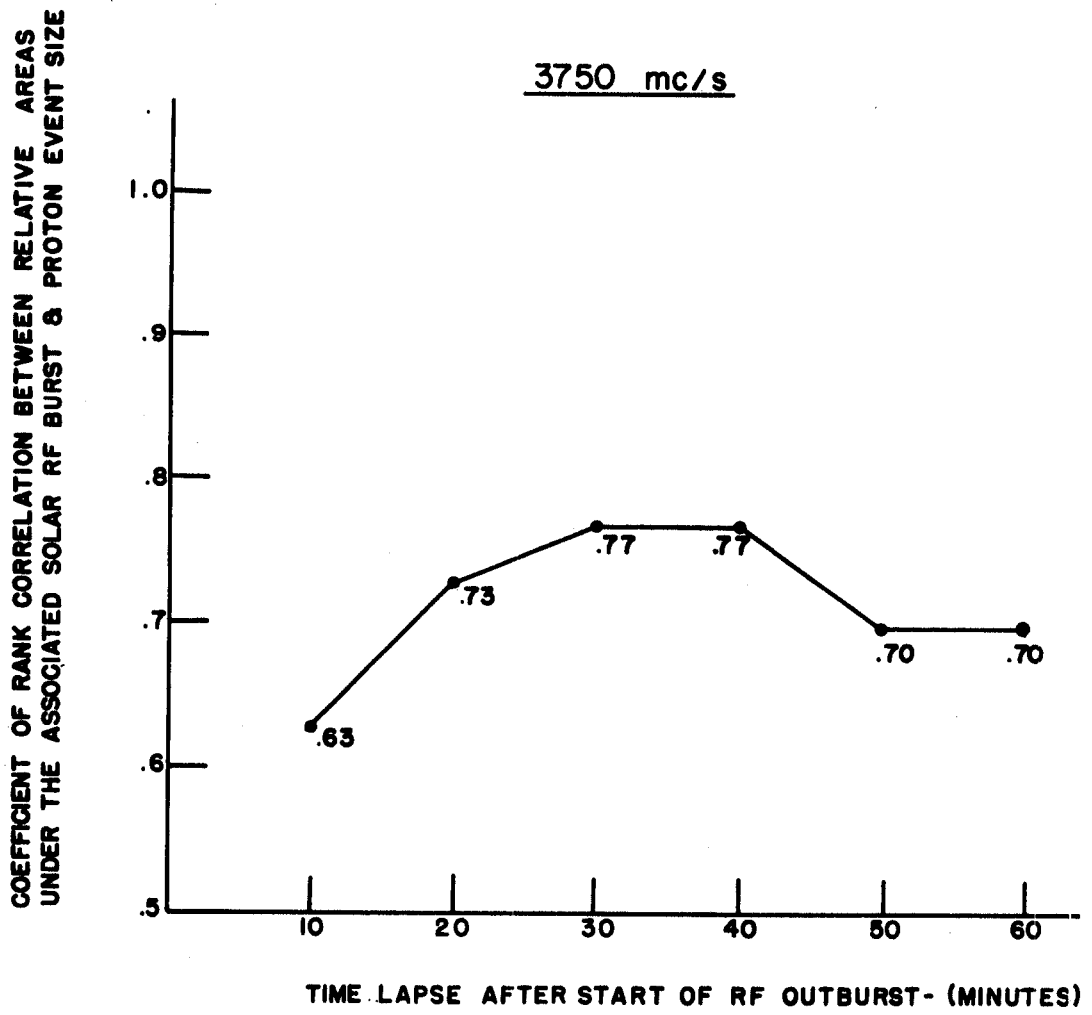

CONCLUSIONS

The results that are presented in this report have certain limitations. First of all, it is not completely certain that every associated solar RF burst that has been chosen was the one that was actually related to the proton emission. The small sample size on which the analysis has been based imposes a statistical limitation. Any possible large errors in the tables and data would be inherent in the analysis. Also there is no absolute assurance that criteria established for large proton events from solar cycle 19 will apply to large proton events occurring in future solar cycles.

Different types of solar radio emission and present models of interplanetary space will be discussed in order to give a more thorough understanding of the relation between solar radio emission and large solar cosmic ray increases. This discussion encompasses the work of several writers and offers an explanation for some of the findings of this study.

Radio emission from the sun has been classified[20-30] into six different types. For a list of the types of solar radio emission and their respective characteristics see Table 1. The only radio emission believed to be of thermal origin is type I.[30] All of these emissions appear to be associated in one way or another with solar flares.[9] In some major flare disturbances all of the radio events are present. Types III and V are simultaneous with the sudden expansion of the flare. A few minutes later type II events may start. Type II is followed by or merges into the start of the type IV bursts, which continue for hours. In this study, primary concern has been with the characteristics of types II and IV emission recorded on fixed frequency records.

The generating mechanisms for each of the types of solar radio emission, have been suggested by several observers.[20-27] J. P. Wild suggests the following sequence of the events:[20]

> "a flare is originated by an explosion near the photosphere; this explosion causes a sudden increase in the emission of H_α light (the flare); ejects a stream of relativistic electrons which escapes immediately into the outer layers of the corona and beyond (III and V type bursts) and sets up a shock-wave which carries with it further relativistic electrons (II and IV type bursts). The physical nature of this postulated explosion is an unsolved problem. Almost 10^{33} relativistic electrons are produced during a flare; the particles follow a spiral path along the lines of force, which are materialized by the coronal streamers and excite the coronal plasma, causing type III bursts. The same relativistic electrons radiate synchrotron radiation causing type V bursts. In several cases the particles escape in the interplanetary space, but in other cases they come back following the lines of force; so we have the U bursts. The shock wave originated by the same explosion moving in the coronal plasma at a velocity of about 1000 km/s (about 10 times the sound velocity in the corona) excited the plasma and causes type II bursts. The magnetic field and relativistic electrons carried by the shock-wave originate type IV bursts."

For several years it has been maintained that certain solar flares are accompanied by the emission of energetic protons.[8, 10, 20, 32-36] The fact that intense radio outbursts accompany these proton increases, and are so closely correlated with them, suggests that the same sources are responsible for the production of the radio emission and the ejection of energetic protons from the sun. However, due to a lack of direct observational data existing at the present time, a clear picture cannot be constructed.[37]

The results of the studies presented here show that there is a delay between the start of the associated RF signal and the start of the PCA event. Present models of the interplanetary space that have received the most attention are those of Parker and Gold. The various arguments[9, 38] that have been presented for and against these models will not be given here. Both models postulate storage of the flare-produced particles in interplanetary space, but the details of the storage mechanism are rather different. It may be of interest to point out that both models, with their postulation of a storage

mechanism, are supported by this delay between the solar radio outbursts and PCA events.

In Parker's model[9, 39-42] a solar wind is assumed. This solar wind is described as a smooth steady flow of gas streaming radially outward from the sun at all times. The solar wind is also believed to stretch any field lines that emerge from the sun. A shock wave from activity on the sun is believed to cause instabilities in the solar wind and consequent disordering of its frozen-in magnetic fields. This forms a magnetic "barrier" somewhere beyond the earth's orbit. When a flare emits a burst of particles, they rapidly fill the region between the sun and the barrier and then slowly diffuse through the barrier. The long decay of the proton event (from 1 to 7 days)[8] seen at the earth represents the slow loss from the inner solar system.

Gold's model[9, 20, 31, 39] assumes that a disturbance on the sun pushes out the solar field in a "tongue" as indicated in Figure 1. The lines of force form closed loops which are anchored at both ends in the solar photosphere. The disturbance does not necessarily result in the acceleration of particles. Such a field configuration can form a "magnetic bottle" in which particles can be trapped for long periods of time. In this model, the particles released by the flare diffuse through the solar atmosphere until they reach a magnetic bottle which happens to extend out to the vicinity of the earth at the time. The bottle then gradually fills with particles. If the earth enters this region, an increase in flux is observed at the earth. The tongues are expected to become detached from the sun after a few days and float away as self-contained magnetic clouds. These plasma clouds are believed to give rise to magnetic storms at the earth.

These magnetic bottles postulated by Gold may serve to explain the false alarms. A false alarm is defined as a case when a characteristic solar radio emission signal is received, but no large

TABLE 13

SOLAR RADIO EMISSION

Type	Duration	Polarization	Associated Optical Features	Wavelength Spectrum	Remarks
I	Hours or days	mainly polarized	Large sunspot groups	1 to 15 m	Noise storms
II	1-10 minutes	Variable	Solar flare	cm, dm, m	Slow-drift bursts
III	Seconds	Variable	Small solar flare	cm, dm, m	Fast-drift bursts
U	Seconds	Variable	Small flare	cm, dm, m	Special case of a Type III burst
IV	Hours	Circular	Solar flare	cm, dm, m	Long continuum bursts
V	Minutes	Circular	Solar flare	cm, dm, m	Short continuum bursts

GOLD'S MODEL OF INTERPLANETARY SPACE

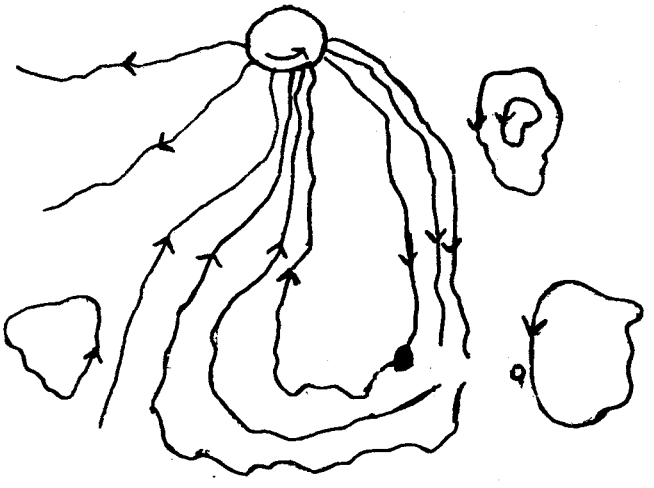

Figure 11
A schematic representation of a tongue of magnetic lines of force drawn out from the sun. The solid circle represents a possible position of the earth within the storage region; the open circle represents a possible position outside the storage region.

associated solar cosmic ray increase is observed at the earth. With a false alarm, copious particle emission may well occur, but the tongue into which the particles diffuse perhaps does not extend as far out as the vicinity of the earth or in a direction away from the earth. When the tongue becomes detached it possibly floats away in such a direction so as not to come in contact with the earth.

Solar cosmic ray increases can be detected indirectly through their effects on the absorption of VHF cosmic noise in the ionospheric D-layer over the polar caps. This is called polar cap absorption (PCA) and is measured by an instrument called a riometer.[1, 8-12, 20, 31, 43] During a solar particle event the earth is bombarded by energetically charged particles. Due to the earth's magnetic field these particles can enter only at high latitudes. By particle interaction the electron density in the upper atmosphere is increased. This increased electron density causes absorption of the galactic radio noise and consequent decrease in the signal measured by the riometer at the ground. The particles primarily responsible for this absorption are protons in the 20-200 Mev kinetic energy range.[8, 12, 43] Particles which are more energetic than 200 Mev ionize so lightly, while passing through the D-layer of the atmosphere, that they are not as effective for the absorption of cosmic radio noise.

The bulk of the solar flare particles occur in the kinetic energy range of 20-200 Mev.[8, 9, 12] Since the riometer is mainly sensitive to protons in this energy range, the start of the PCA events may be taken as the arrival time for the proton hazard to space flight.

Large solar cosmic ray increases are a danger to space flight.[8-12, 42-50] The total radiation dose from one of these events difinitely presents a hazard to future space travelers. The radiation effects on materials, electronic components, and other instruments used in space missions also present a problem. Consequently, a solution to this problem must be found before further penetration of

space is attempted.

One of the areas where a possible solution to the space radiation problem may be found is the field of warning. A "warning" is the indication of a large solar proton event, which has already occurred, before the arrival of the corpuscular radiation. In the case of an interplanetary mission, once a warning is given that a stream of particles from a solar radiation event is headed toward the space craft, various precautionary measures may be taken. To protect the space travelers and sensitive instruments, spot shielding, near body shielding, shadow shielding, artificially generated magnetic fields around the space craft, and a variety of other techniques can be used.[11, 12, 45-48]

There are many indications that a warning of solar proton events may be provided by means of a scientific system which uses selective criteria on the characteristics of associated phenomena to these events. The results presented in this report can serve as the basic criteria for an electronic system that may provide such a warning. Specific signal characteristics of solar RF emission which are indicative of large proton events, can be built into an electronic proton warning system. Since the RF signal characteristics specified in this study precede the start of the PCA event in every case, then such a warning system would give an alarm before the arrival of the actual proton hazard. A system of this type would not be overly complex and can possibly be operated in the future both from the ground and on a manned space craft.

This study of the relationship between solar radio emission and large solar proton events has indicated the following:

1. There is a good correlation between specific signal characteristics of solar RF emission outbursts and large solar proton events.
2. A P(A/N) of 100% can be obtained with the signal characteristics of duration and maximum flux density.
3. The frequencies in the range 1000-3750 mc/s, with the frequencies 1000, 2000, 2800, and 3750 mc/s in particular, are perhaps the most reliable for the indication of large proton events.

4. The false alarms can be reduced in number, and thus, the P(N/A) increased, by consideration of additional solar RF emission signal characteristics.
5. The optimum situation, with respect to the P(A/N) and P(N/A) is obtained when signal characteristics are specified on a combination of fixed frequencies rather than on only one frequency.
6. To retain a maximum P(A/N), the P(N/A) cannot be appreciably increased beyond 57%.
7. The false alarms are a permanent phenomena.
8. For large proton events the minimum delay time between the start of the associated RF signal and the start of the PCA event is 25 minutes, the maximum is 826 minutes, and the mean is 178 minutes. There is a tendency toward the occurence of the shorter delay time.
9. The signal characteristics (optimum frequencies) specified for the indication of large proton events can be detected prior to the start of the PCA event in every case.
10. When the area under the associated RF signal for specific times is compared with the proton event size, there is an indication of a relationship.
11. Both Parker's and Gold's model of the interplanetary fields offer an explanation for some of the basic findings of the analysis.
12. The results of the analysis can serve as the basic criteria for an electronic system that may provide a warning for large proton events.
13. An RF proton event warning system would not be overly complex and could be operated both from the ground and on a manned space craft.

14. Analysis of the relationship between other associated phenomena (solar flares, solar ultraviolet and x-rays, solar magnetic fields, and interplanetary fields) and large proton events may result in additional criteria for a warning system.
15. An RF system would probably be the most efficient (in terms of reliability, versatility, economy, and atmospheric effects) for proton event warning.

LIST OF REFERENCES

1. Warwick, Constance S. and Haurwitz, Marion Wood, A Study of Solar Activity Associated With Polar-Cap Absorption, (Journal of Geophysical Research, Vol. 67, No. 4, 1962)

2. Malville, J. M. and Smith, S. F., Type IV Radiation From Flares Covering Sunspots, (Journal of Geophysical Research, Vol. 68, No. 10, 1963)

3. Bracewell, Ronald N. (ed.), Paris Symposium on Radio Astronomy, (Stanford University Press, Stanford, California, 1959) pp. 210-213

4. Bell, Barbara, Solar Radio Bursts of Spectral Types II and IV: Their Relations to Optical Phenomena and to Geomagnetic Activity, (Smithsonian Contributions to Astrophysics, Vol. 5, No. 15, 1963)

5. Sakurai, K. and Maeda, H., A Relation Between Solar Radio Emission and Low-Energy Solar Cosmic Rays, (Journal of Geophysical Research, Vol. 66, No. 6, 1961)

6. Kundu, M.R., Some Relations between Centimeter-Wave Radio Bursts and Solar Cosmic Rays and X-rays, (Journal of Geophysical Research, Vol. 66, No. 6, 1961)

7. Maxwell, A., Howard, W.E., III, and Garmire, G., Some Statistics of Solar Radio Bursts at Sunspot Maximum(Journal of Geophysical Research, Vol. 65, No. 11, 1960)

8. McDonald, Frank B. (ed.) Solar Proton Manual, (Goddard Space Flight Center, X-611-62-122, Greenbelt, Md., 1963)

9. Legalley, Donald P. (ed.) Space Science, (John Wiley and Sons, Inc., New York, 1963) pp. 112-122, 169-172, 180-186, 406-409, 427-445, 474-477, 515-520

10. Smith, Henry J. and Smith, Elske, V. P. Solar Flares, (MacMillan Co., New York, 1963) pp. 177-229.

11. Pay, Rex, Apollo Astronauts are Painstakingly Protected from Solar-Flare Protons, (Missiles and Rockets, Vol. 15, No. 3, 1964)

12. "Protection Against Radiation Hazards in Space," (U.S. Atomic Energy Commission, TID-7652, 1962) pp. 12-375, 662-682, 794-829

13. Gill, W.L., Analysis of Solar Proton Events to Determine the Radiation Flux Exposure for Manned Space Flight, (Nasa TN, 1962)

14. Noyes, John C., Solar Active Regions and Solar Cosmic Rays, (Journal of the Physical Society of Japan, Vol. 17, Supp. A-II, 1962)

15. Chupp, E.L., and Williams, R.W., Intensity of Solar Proton Emissions, (Journal of the Physical Society of Japan, Vol. 17, Sup. A-II, 1962)

16. Sarabhai, V.A., and Pai, G.L., Cosmic Ray Effects Associated with Polar Cap Absorption Events, (Journal of the Physical Society of Japan, Vol. 17, Supp. A-II, 1962)

17. Tanaka, Dr. Haruo, Chief of the Radio Astronomy Section, The Research Institute of Atmospherics, Nagoya University, Toyokawa, Aichi, Japan, May 10, 1963, Personal Letter

18. Covington, Arthur E., Chief of the Radio Astronomy Section, Radio and Electrical Engineering Division, National Research Council, Ottawa, Canada, May 22, 1963. Telephone Conversation

19. Spiegel, Murray R., Theory and Problems of Statistics, (Schaum Publishing Co.. New York, 1961) p. 246

20. Peters, B. (ed.), Cosmic Rays, Solar Particles, and Space Research, (Academic Press, New York, 1963) pp. 8-30, 57

21. Brown, R. Hanbury and Lovell, A.C.B., The Exploration of Space by Radio, (John Wiley and Sons, Inc., New York 1958) pp. 121-126

22. Steinberg, Jean Louis and Lequeux, James, Radio Astronomy, (McGraw-Hill, New York 1963) pp. 136-159

23. Maxwell, A., Recent Developments in Solar Radio Astronomy, (Proceedings of the National Academy of Sciences, Vol. 46, No. 9, 1960)

24. Menzel, Donald H. (ed.), The Radio Noise Spectrum, (Havard University Press, Cambridge, Mass., 1960) pp. 101-110

25. Uchida, Yutaka, On the Exciters of Type II and III Solar Radio Bursts, (Journal of the Physical Society of Japan, Vol. 17, Supp. A-II, 1962)

26. Wild, J.P., The Radio Emission from Solar Flares, (Journal of the Physical Society of Japan, Vol. 17, Supp. A-II, 1962)

27. Kuiper, Gerard P. (ed.), The Sun, (The University of Chicago Press, Chicago, Illinois, 1953) pp. 466-528

28. Piddington, J.H., Radio Astronomy, (Harper and Brothers, New York 1961) pp. 85-105

29. Modisette, Jerry D., The Electromagnetic-Radiation Environment of a Satellite, (Nasa TN D-1361, 1962)

30. Abetti, Giorgio, Solar Research, (Macmillan Co., New York, 1963) pp. 138, 149-152

31. Aarons, J. and Silverman, S.M. (ed.), AFCRL Studies of the November 1960 Solar-Terrestrial Events, (U.S. Air Force Pub. 62-441, 1962) pp. 21-26, 37-45, 66

32. Wolfendale, A.W., Cosmic Rays, (Philosophical Library, Inc., New York, 1963) pp. 155, 163-169

33. Davies R.D. and Palmer, H.P., Radio Studies of the Universe, (Routledge and Kegan Paul Ltd., London, 1959) pp. 116-129

34. Waldmeier, M., Optical Evidence for Corpuscular Radiation of the Sun, (Journal of the Physical Society of Japan, Vol. 17, Supp. A-II, 1962)

35. Wilson, B.G. and Hehra, C.P., Cosmic Ray Increases Associated with Solar Flares, (Journal of the Physical Society of Japan, Vol. 17, Supp. A-II, 1962)

36. Warwick, James W., The Sources of Solar Flares, (Publications of the Astronomical Society of the Pacific, Vol. 74, No. 439, 1962)

37. Deutsch, Armin J. and Klemperer, Wolfgang, B., (ed.), Space Age Astronomy, (Academic Press, New York, 1962) pp. 169, 189-193

38. Warwick, Constance S., Solar Particles and Interplanetary Fields, (AAS Preprint No. 63-33, 1963)

39. Reid, George O., A Diffusive Model for the Initial Phase of a Solar Proton Event, (Journal of Geophysical Research, Vol. 69, No. 13, 1964)

40. Liller, William (ed.), Space Astrophysics, (McGraw-Hill, New York, 1961) pp. 157-170

41. Berkner, Lloyd V. and Odishaw, Hugh (ed.), Science in Space, (McGraw-Hill, New York, 1961)

42. Rosen, A. Eberhard, C.A., Farley, T.A., Vogl, J.L., A Comprehensive Map of the Space Radiation Environment, (U.S. Air Force AF41(609)-1456, 1962) pp. 87-114, 121-123, 225-229

43. "Lunar and Planetary Exploration," (North American Aviation PUB. 513-W-12, 1962) pp. 53-74, 99, 117-134

44. Shlanta, A., A Statistical Analysis of Solar Proton Event Data, (IOL 224-130-63-015, North American Aviation Inc., 1963)

45. Wallner, Lewis E. and Kaufman, Harold R., Radiation Shielding for Manned Space Flight, (Nasa TN-681, 1961)

46. Saylor, W.P., Winter, D.E., Eiwen, O.J., and Caraiker, A.W., Space Radiation Guide, (U.S. Air Force AMRL-TDR-62-86, 1962)

47. "Apollo Radiation Shielding Status Report," (SID 62-821 North American Aviation Inc., 1962)

48. Keller, J.W., A Study of Shielding Requirements for Manned Space Missions, (NASA Contract Nasa-50, 1960) pp. 33-38, 43-51, 77-80

49. Malitson, Harriet H., Predicting Large Solar Cosmic Ray Events, (Astronautics and Aerospace Engineering, Vol. 1, No. 2, 1963)

50. Bouquet, Frank L. Jr., The Radiation Hazard of Space, (Astronautics and Aerospace Engineering Vol. 1, No. 2, 1963)

APPENDIX 1

SOLAR RADIO EMISSION OUTBURSTS ASSOCIATED WITH LARGE PROTON EVENTS

No.	Date	Sta.	Freq.	Start Time U.T.	Time of Max U.T.	Dura.	Max. Flux Dens. Inst. 10^{-22} wm^{-2}	Max. Flux Dens. Smooth (c/s)$^{-1}$	Proton Event Size E > 30 Mev
1.	2-23-56	Tok	3000	0333		50.0	>4700	>4410	1.6 x 10^9
		Nag	3750	0334		15.5			
		Tok	200	0335		25.0	>2000	>5000	
2.	1-20-57	Cav	81	1056					3 x 10^8
		Pra	536	1057		93.0	>280	90	
		Ned	2980	1100		24.0	184	138	
3.	7-3-57	Pra	536	0714		156.5	>282	>120	1 x 10^7
		Ucc	600	0722		38.0	113	33	
		Nag	1000	0723	0809.7	60.0		7570	
		Gor	9375	0725		35.0	600		
		Nag	2000	0726	0809.5	50.0		1690	
		Ned	2980	0726.5		31.0	585	152	
		Nag	3750	0727	0742	45.0		337	
		Hhi	9400	0729	0841	121.0		2380	
		Jod	80	0730	0745	>15.0	54	>28	
		Nag	9400	0730	0742	45.0		196	
		Gor	3000	0733		30.0	285		
		Tok	9500	0733x	0742		710	231	
		Aop	231	0750	0810	40.0	700	550	
		Ned	200	0802.5		1.5	300	120	
		Ned	545	0805		14.5	850	300	
4.	8-31-57	Tok	200	0540x	0615x	60.0	830	290	1 x 10^7
		Tok	3000	0545.5x	0549x	>3.5	569	221	
		Tok	9500	0546.7x	0548.3	>0.6	696	241	
		Nag	2000	0548x	0549	80.0		164	
		Nag	3750	0548x	0548	60.0		261	
		Nag	1000	0548	0549	100.0		285	
		Nag	9400	0548	0548	22.0		195	
		Ucc	169	0548		4.0	>350		
		Tok	200	0548	0549.5	4.0	1600	270	
		Ned	545	0548		102.0	>4000	2000	
		Syd	1420	0548	0549	2.0	214	156	
		Ned	2980	0548		12.0	426	44	
		Syd	600	0549	0550	2.0	104	30	
		Syd	600	0557	0654	93.0	455	196	
5.	8-31-57	Jod	80	1300	1305	10.0	132	44	
		Jod	200	1300	1310	15.0	>200	>118	
		Nbs	450	<1300	1338	180.0	>14000	>8500	
		Ott	2800	1301	1315.5	65.0		3900	
		Hhi	9400	1302		170.0		>900	
		Ucc	169	1303		12.0	>300		
		Ned	200	1303		13.0	>1200	400	
		Aop	231	1303	1307	15.0	>1400	1250	
		Ucc	169	1315		2.0	>300		
6.	10-20-57	Nbs	167	1600.6	1601	0.5	2000		1 x 10^7
		Ott	2800	1644	1651	51.0		4000	
		Nbs	167	1646	1700	89.0	>3700	650	
		Nbs	450	1647	1656	43.0	>14000	>7000	

No.	Date	Sta.	Freq.	Start Time U.T.	Time of Max U.T.	Dura.	Max. Flux Dens. Inst. 10^{-22} wm^{-2}	Max. Flux Dens. Smooth (c/s)$^{-1}$	Proton Event Size E > 30 Mev
7.	3-23-58	Ned	2980	0953		110.0	>1340	536	4×10^8
		Aba	209	0957	1003	12.0	182		
		Aba	209	0957	1003	123.0			
		Aop	231	0957.3	0958.4	1.2	800	200	
		Jod	3000	0958	1002	10.0	>1190	>655	
		Sim	208	1000	1005	15.0	430	250	
		Ucc	600	1001		17.0	1000		
		Cra	810	1001	1012	111.0	650	80	
		Irs	169	1002		14.4	>90	>77	
		Osl	200	1002	1006	8.5	1000	400	
		Mos	208	1002	1006	98.0	1890	1020	
		Aop	23	1003	1003.2	1.0			
		Ucc	169	1003		239.0			
		Cav	178	1003		8.5		>65	
		Jod	200	1003	1007	7.0	>240	>216	
		Ned	545	1003		100.0	>360	120	
		Jod	80	1005	1008	15.0	>140	>140	
		Cav	178	1010		180.0	>65	35	
		Gor	207	1012	1025	110.0	130	34	
		Kis	178	1014	1034	58.0	140		
		Cav	81	1020		90.0	>45	3	
		Ucc	169	1022		45.0	>100		
8.	7-7-58	Nag	1000	0026.5	0028	5.0	1370	1000	5×10^8
		Ott	2800	0026.5	0027.5	>8.5		875	
		Tok	9500	0026.7	0028x	12.0	1303	877	
		Tok	200	0026.9	0027.1	3.0	4000	1600	
		Hir	200	0027	0028	120.0	1620	400	
		Hol	545	0027		120.0	350	140	
		Nag	2000	0027x	0028	10.0		550	
		Nag	3750	0027	0028	10.0		990	
		Syd	600	0028	0028	1.0	145	85	
		Tok	200	0033	0035.5	3.0	300	250	
		Syd	600	0040	0043	92.0	129		
		Nag	2000	0040	0041.3	4.0		40	
		Nag	1000	0041	0042	3.0		140	
		Syd	1420	0041	0113	91.0	827		
		Tok	3000	0050.2	0111.3	100.0	3770	3432	
		Nag	2000	0055	0111.5	38.0		1300	
		Tok	9500	0055	0111.8	70.0	1910	1430	
		Tok	200	0100	0153x	90.0	900	730	
		Nag	1000	0101	0112	60.0		800	
		Nag	3750	0102.5x	0111.4	30.0		1700	
		Nag	9400	0103.5x	0111.4	30.0		920	
		Tok	200	0235.7		0.3	4000	4000	
9.	8-16-58	Ucc	600	0430		93.0	180		2×10^7
		Nag	2000	0434	0440	60.0		2900	
		Tok	3000	0434	0440	70.0	5030	4794	
		Nag	3750	0434	0439	60.0		5800	
		Tok	9500	0434	0440	70.0	7340	6920	

No.	Date	Sta.	Freq.	Start Time U.T.	Time of Max U.T.	Dura.	Max. Flux Dens. Inst. 10^{-22} wm^{-2}	Max. Flux Dens. Smooth $(c/s)^{-1}$	Proton Event Size E > 30 Mev
		Nag	1000	0435	0442	85.0		4800	
		Syd	1420	0436	0440	17.0	1089	416	
		Hol	200	0438		57.0	>200	>150	
		Ucc	169	0439		5.0	3500		
		Tok	200	0440x	0440.5	3.0	18000	18000	
		Syd	600	0440	0530	80.0	224	89	
		Tok	200	0443	0501	30.0	2300	1900	
		Ucc	169	0444		36.0	2650	960	
		Syd	1420	0453	0515	59.0	659	366	
		Pra	536	0537	0547.5	26.0	180	120	
		Syd	1420	0537	0537	1.0	549	350	
		Ucc	169	0614		4.0	75	35	
10.	8-22-58	Hhi	9400	1423	1451	172.0	718		5×10^7
		Hhi	1500	1427	1509	128.0	443		
		Ott	2800	1430	1506	120.0		1500	
		Ucc	169	1432		208.0	540		
		Ucc	600	1432		73.0	306	130	
		Aop	231	1436	1503	214.0	1800	700	
		Ned	545	1437		86.0	190	30	
		Cor	201	1438.5		0.5	180	120	
		Ned	200	1440		135.0	1400	300	
		Nbs	167	1444	1508	121.0	2000	730	
11.	8-26-58	Nag	2000	0005	0042	57.0		2100	5.3×10^7
		Nag	3750	0005	0041	50.0		5050	
		Nbs	167	0016x	0127	>69.0	>2400		
		Syd	1420	0016	0042	89.0	288	91	
		Syd	600	0017	0102	89.0	85	48	
		Nag	1000	0017	0022	59.0	1900	1600	
		Tok	9500	0018	0026	60.0	5920	5475	
		Hol	200	0019		120.0	85000	26000	
12.	5-10-59	Ott	2800	2100	2149	>160.0		2500	1.2×10^9
		Hol	545	2104.5		4.5	>330	120	
		Nbs	167	2107.6	2107.6	0.2	>100		
		Nbs	167	2111.8	2112	0.2	>100		
		Hir	200	2114.2	2115.1	1.3	910	230	
		Nbs	167	2115		>275.0	>1000		
		Nbs	167	2115	2122	6.9	>1000		
		Hol	545	2116		150.0	450	300	
		Tok	9500	<2117	2149	>60.0	2900	2400	
		Hir	200	2120	2148	135.0	390	200	
		Nbs	167	2122	2141	>18.0	>1000		
		Hir	200	2122.7	2123	1.0	1050	150	
		Nag	1000	<2200	2222	>100.0		1550	
		Nag	2000	<2200	2213	>100.0		1300	
		Nag	9400	<2200	2203	>100.0		1650	
13.	7-10-59	Haw	200	0200	0200.1	2.0			8×10^8
		Hol	545	0208		32.0	1000	300	
		Nag	1000	0209	0223	100.0	6000	4750	
		Nag	3750	<0209	0224	>38.0		6300	
		Nag	9400	<0209	0224	>36.0		26500	
		Nag	2000	<0211	0224	>90.0		3000	

No.	Date	Sta.	Freq.	Start Time U.T.	Time of Max U.T.	Dura.	Max. Flux Dens. Inst. $10^{-22}wm^{-2}(c/s)^{-1}$	Max. Flux Dens. Smooth $10^{-22}wm^{-2}(c/s)^{-1}$	Proton Event Size E>30 Mev
		Irk	209	0209	0221	56.0	>1400	30	
		Nbs	167	0210	0210	5.0	>1000		
		Syd	600	0244		>60.0	>252		
		Irk	209	0318	0345	100.0	44	28	
14.	7-14-59	Syd	1420	0330		131.0	>114		$2x10^9$
		Nag	3750	0330	0356	100.0		6000	
		Nag	9400	0330	0349	65.0		6300	
		Nag	1000	0331	0422	125.0	20600	4900	
		Nag	2000	0331	0420	125.0		8450	
		Hol	200	0337		600.0	10000	300	
		Hol	545	0337		125.0	40000	4000	
		Tor	127	<0600	0900	>540.0	100	80	
15.	7-16-59	Hol	545	2114		165.0	5500	1000	$3x10^9$
		Ott	2800	2118	2154	>180.0		6500	
		Hol	200	2120		250.0	1100	150	
		Nbs	167	2121	2121.6	2.0	>1000		
		Nbs	167	2123	2124	>287.0	>1000		
		Nag	2000	<2201	2210	>65.0		2350	
		Nag	3750	<2201	2201	>60.0		1500	
		Nag	1000	<2204	2226	>65.0		6500	
		Nag	9400	<2207	2207	>45.0		640	
							Peak	Mean	
16.	4-28-60	Tok	9500	0124.5	0130	15.0	573	208	$2.5x10^7$
		Nag	3750	0116	0129.5	40.0	260		
		Nag	2000	0115	0129.7	30.0	285		
		Nag	1000	0117	0139.2	25.0	265		
		Hol	545	0135		5.0	170	50	$4x10^7$
17.	9-3-60	Nag	9400	0039	0108	75.0	$1.47x10^4$		
		Nag	3750	0039	0104.6	85.0	$1.2x10^4$		
		Nag	2000	0035	0105.2	90.0	7100		
		Nag	1000	0035	0105.6	90.0	3770		
		Tok	9500	0103.7	0108	33.0	7000		
		Tok	3000	0059		50.0	5600		
		Hol	545	0103.5		17.0	>180	>180	
		Hir	200	0103		33.0	>1000	>1000	
18.	11-12-60	Ned	9100	1322	1332	100.0	>7500	3750	$2.7x10^9$
		Ott	2800	1320	1345.5	340.0	5500		
		Hhi	1500	1323	1328.7	>90.0	770		
		Pra	808	1325	1341	80.0	>240		
		Ned	545	1326.5		100.0	>5000	1000	
		Ned	200	1327.5		270.0	>2000	300	
19.	11-15-60	Nag	9400	0218	0228.4	85.0	24000		$2x10^9$
		Nag	3750	0219	0222	80.0	11600		
		Nag	2000	0220	0222.6	75.0	4950		
		Nag	1000	0220	0227.1	235.0	8600		
		Hol	545	0221.5		160.0	800	60	
		Hol	300	0221		238.0	>2700	160	

No.	Date	Sta.	Freq.	Start Time U.T.	Time of Max U.T.	Dura.	Max. Flux Dens. Peak $10^{-22}wm^{-2}(c/s)^{-1}$	Mean	Proton Event Size E>30 Mev
20.	11-20-60	Ott	2800	2023	2026.5	>47.0	400		$6x10^7$
		Par	545	2025		50.0	90	40	
		Par	200	2028		5.0	220	100	
		Nbs	108	2027.5	2033	7.0	>300		
		Nbs	108	2038	2039,9	15.0	300		
		Nbs	18	2042		2.0			
21.	7-12-61	Ned	9100	1018	1029	87.0	6000	1500	10^7
		Ned	2980	1018		87.0	4100	1100	
		Ott	2800	1145		225.0	45	13	
		Hhi	1500	1010	1042.5	240.0	1700		
		Ucc	600	1019		100.0	950	250	
		Ned	200	1022		80.0	22000	2000	
		Aop	111	1024.2	1030	96.0	4000	350	
		Aop	23	1023.8	1031.4	28.5	3000	300	
22.	7-18-61	Ned	9100	0939		70.0	>>2400		$2.5x10^8$
		Ned	2980	0938		65.0	2400	800	
		Hhi	1500	0938.5	0958	231.5	1180		
		Pra	808	0943		77.0	300		
		Ned	545	0944		50.0	650	200	
		Ned	200	0944		60.0	1000	200	
		Aop	111	0944	0956.7	226.0	4000	150	
		Aop	23	0946.2	0951.5	44.0	3000	300	
23.	9-28-61	Nag	9400	2213	2217.3	40.0	1600		10^7
		Nag	3750	2212	2217.3	40.0	1690		
		Nag	2000	2211	2220.2	40.0	1000		
		Nag	1000	2208		45.0	>>75		
		Hol	545	2214		36.0	1600	300	
		Hol	200	2213		9.0	>900	150	
		Nbs	108	2213	2217	9.0	>300		
		Nbs	108	2222	2347	102.0	>300		
		Nbs	18	2214		54.0			
		Ott	2800	2211	2318	>30.0	800		

APPENDIX II

MIXED FREQUENCY SOLAR RADIO EMISSION OUTBURSTS ASSOCIATED WITH LARGE PROTON EVENTS

No.	Date	Sta.	Freq.	Start Time U.T.	Time of Max U.T.	Dura.	Max. Flux Dens. 10^{-22} wm^{-2}(c/s)$^{-1}$ Inst.	Smooth	Proton Event Size E>30 Mev
1.	7-3-57	Nag	1000	0723	0809.7	60		7570	10^7
		Nag	2000	0726	0809.5	50		1690	
		Nag	3750	0727	0742	45	337		
2.	8-31-57	Nag	1000	0548	0549	100		285	10^7
		Nag	2000	0548	0549	80		164	
		Nag	3750	0548	0548	60	261		
3.	7-7-58	Nag	1000	0101	0112	60		800	$5x10^8$
		Nag	2000	0027	0028	10		550	
		Nag	2000	0055	0111.5	38		1300	
		Nag	3750	0102.5	0111.4	30		1700	
		Nag	3750	0027	0028	10		990	
4.	8-16-58	Nag	1000	0435	0442	85		4800	$2x10^7$
		Nag	2000	0434	0440	60		2900	
		Nag	3750	0434	0439	60		5800	
5.	8-26-58	Nag	1000	0017	0022	59	1900	1600	$5.3x10^7$
		Nag	2000	0005	0042	57		2100	
		Nag	3750	0005	0041	50		5050	
6.	5-10-59	Nag	1000	<2200	2222	>100		1550	$1.2x10^9$
		Nag	2000	<2200	2213	>100		1300	
		Nag	3750	<2200	2203	>100		1650	
7.	7-10-59	Nag	1000	0209	0223	100	6000	4750	$8x10^8$
		Nag	2000	<0211	0224	>90		3000	
		Nag	3750	0209	0224	>38		6300	
8.	7-14-59	Nag	1000	0331	0422	125	20600	4900	$2x10^9$
		Nag	2000	0331	0420	125		8450	
		Nag	3750	0330	0356	100		6000	
9.	7-16-59	Nag	1000	<2204	2226	>65		6500	$3x10^9$
		Nag	2000	<2201	2210	>65		2350	
		Nag	3750	<2201	2201	>60		1500	
							Peak	Mean	
10.	4-28-60	Nag	1000	0117	0139.2	25		265	$2.5x10^7$
		Nag	2000	0115	0129.7	30	285		
		Nag	3750	0116	0129.5	40	260		
11.	9-3-60	Nag	1000	0035	0105.6	90	3770		$4x10^7$
		Nag	2000	0035	0105.2	90	7100		
		Nag	3750	0039	0104.6	85	$1.2x10^4$		
12.	11-15-60	Nag	1000	0222	0227.1	235	8600		$2x10^9$
		Nag	2000	0220	0222.6	75	4950		
		Nag	3750	0219	0222	80	11600		
13.	9-28-61	Nag	1000	2208		45	>>75		10^7
		Nag	2000	2211	2220.2	40	1000		
		Nag	3750	2212	2217.2	40	1690		

APPENDIX III

MIXED FREQUENCY SOLAR RADIO EMISSION

OUTBURSTS ASSOCIATED WITH SMALL EVENTS

No.	Date	Sta.	Freq.	Start Time U.T.	Time of Max U.T.	Dura.	Max. Flux Dens. 10^{-22} wm^{-2}(c/s)$^{-1}$ Inst.	Smooth	Proton Event Size E>30 Mev
1.	6-6-58	Nag	1000	0433	0446.1	40		263	10^6
		Nag	2000	0433	0447.2	26	420		
		Nag	3750	0433	0450.2	28		360	
							Peak	Mean	
2.	3-29-60	Nag	1000	0656	0812.8	120	2.47×10^5		3.6×10^{8}*
		Nag	2000	0655	0733.4	120	4.9×10^4		
		Nag	3750	0655	0733.5	52	8250		
3.	4-5-60	Nag	1000	0136	0302.8	135	18000		1.1×10^6
		Nag	2000	0140	0206.1	125	1230		
		Nag	3750	0140	0202.3	90	6000		
4.	4-29-60	Nag	1000	0139	0207.3	82		3.03×10^4	7×10^6
		Nag	1000	0348	0442.2	75	340		
		Nag	1000	0525	0536	23	3350		
		Nag	2000	0232.5	0247.7	30	185		
		Nag	2000	0356	0427.4	50	370		
		Nag	2000	0525	0538.1	23	990		
		Nag	3750	0356	0359.7	55	365		
5.	5-13-60	Nag	1000	0517.5	0556.8	122	2200		4×10^6
		Nag	2000	0417	0557.8	122	1440		
		Nag	3750	0517	0532	105	3750		

*Bailey (E>20 Mev)

APPENDIX IV

MIXED FREQUENCY SOLAR RADIO EMISSION
OUTBURSTS ASSOCIATED WITH NO PROTON EVENTS

No.	Date	Sta.	Freq.	Start Time U.T.	Time of Max U.T.	Dura.	Max. Flux Dens. $10^{-22}wm^{-2}(c/s)^{-1}$ Inst.	Smooth	Proton Event Size E>30 Mev
1.	9-11-57	Nag	1000	0235	0320	70		8200	
		Nag	2000	0243	0304	70		564	
		Nag	3750	0243	0304	90		373	
2.	10-21-58	Nag	1000	2321	2356	55		530	
		Nag	2000	2323	2355	55		520	
		Nag	3750	2323	2327	55		1150	
3.	12-23-58	Nag	1000	0534	0544	70		158	
		Nag	2000	0534	0605	65		370	
		Nag	3750	0534	0605	50		1020	
4.	2-12-59	Nag	1000	2304	2333	40		325	
		Nag	2000	2250	2314	55		335	
		Nag	3750	2250	2313	70		440	
							Peak	Mean	
5.	8-11-60	Nag	1000	0223	0253.3	35	175		
		Nag	2000	0223	0253	35	375		
		Nag	3750	0222	0252.9	35	610		
6.	10-11-60	Nag	1000	0519.5	0524.7	40	310		
		Nag	2000	0523	0527.6	26	630		
		Nag	3750	0520	0532.8	40	1580		
7.	11-14-60	Nag	1000	0259	0336.1	140	1400		
		Nag	2000	0258	0443.7	140	1800		
		Nag	3750	0258	0354.6	140	4300		